

8-2021

Investigation of Cell Behavior in 3D Printed Lumen Structures for Capillary Regeneration

Victoria Jade Perez
The University of Texas Rio Grande Valley

Follow this and additional works at: <https://scholarworks.utrgv.edu/etd>



Part of the [Manufacturing Commons](#)

Recommended Citation

Perez, Victoria Jade, "Investigation of Cell Behavior in 3D Printed Lumen Structures for Capillary Regeneration" (2021). *Theses and Dissertations*. 934.
<https://scholarworks.utrgv.edu/etd/934>

This Thesis is brought to you for free and open access by ScholarWorks @ UTRGV. It has been accepted for inclusion in Theses and Dissertations by an authorized administrator of ScholarWorks @ UTRGV. For more information, please contact justin.white@utrgv.edu, william.flores01@utrgv.edu.

INVESTIGATION OF CELL BEHAVIOR IN 3D PRINTED LUMEN STRUCTURES FOR
CAPILLARY REGENERATION

A Thesis

by

VICTORIA JADE PEREZ

Submitted to the Graduate College of
The University of Texas Rio Grande Valley
In partial fulfillment of the requirements for the degree of

MASTER OF SCIENCE IN ENGINEERING

August 2021

Major Subject: Manufacturing Engineering

INVESTIGATION OF CELL BEHAVIOR IN 3D PRINTED LUMEN STRUCTURES FOR
CAPILLARY REGENERATION

A Thesis

by

VICTORIA JADE PEREZ

COMMITTEE MEMBERS

Dr. Jianzhi Li

Chair of Committee

Dr. Andrew Tsin

Committee Member

Dr. Xiaoqian Fang

Committee Member

Dr. Douglas Timmer

Committee Member

August 2021

Copyright 2021 Victoria Perez
All Rights Reserved

ABSTRACT

Perez, Victoria Jade, Investigation of Cell Behavior In 3d Printed Lumen Structures for Capillary Regeneration. Master of Science in Engineering (MSE), August, 2021, 55 pp., 5 tables, 18 figures, 67 titles.

This thesis work successfully generated a coaxial printing setup and process to generate 3D printed tubules. A dual syringe pump mechanism was developed to print tubular structures to investigate cell behavior with a goal to generate future capillary beds. The mechanism involves the use of collagen - alginate tubules and the use of EDTA to increase the porosity of the tubule structures to study their interaction with media and incubation techniques as well as behavior and morphology. Tubules of 1.7% sodium alginate and 0.4% collagen I reacting with 3.2% CaCl₂ solution proved to be more stable in both the printing process and the incubation process than 0.25% bioink mixes. Migration conforming to the edges of tubule walls, and cell morphology was observed in and outside the tubules showing cells EDTA and collagen were not statistically significant in determining cell viability. Cell behavior within and outside the tubule structures varied and maintained the possibility of utilizing coaxially printed tubules within the designed device to further maintain the tubule and advance the complexity of the cell populations that interact with it.

DEDICATION

The completion of my thesis studies would not have been possible if it were not for the support and patience of my professors, colleagues, and family members. I would like to dedicate the completion of this thesis to my family, and my teachers.

ACKNOWLEDGMENTS

I will always be grateful to Dr. Li, Dr. Tsin, Dr. Fang, and Dr. Timmer for being wonderful teachers and for their guidance. I would like to acknowledge all of my coworkers especially Tuba, Reanna, and Laura for helping with lab and research procedures.

TABLE OF CONTENTS

	Page
ABSTRACT	iii
DEDICATION.....	iv
ACKNOWLEDGMENTS.....	v
TABLE OF CONTENTS.....	vi
LIST OF TABLES.....	viii
LIST OF FIGURES	ix
CHAPTER I. INTRODUCTION.....	1
ADDITIVE MANUFACTURING.....	1
3DBIOPRINTING	2
3D BIOPRINTING AND VASCULATURE	3
APPROACHING THE INCORPORATION OF VASCULATURE.....	5
CHAPTER II. REVIEW OF LITERATURE.....	7
VASCULATURE.....	7
VESSELS	9
CAPILLARIES.....	10
ANGIOGENESIS AND VASCULOGENESIS	11
BIOINK PROPERTIES.....	11

3D BIOPRINTING PROCESSES AND TUBULES	17
POSSIBLE SIMILAR TECHNOLOGIES OR CONCEPTS	19
OVERALL	19
CHAPTER III. METHODOLOGY AND MATERIALS.....	22
CULTURING CELLS, AND STOCK SOLUTIONS.....	22
BIOINK FORMULATION	23
PRINTER & WELL SETUP.....	23
PRINTING.....	23
PRINTING TUBULES AND WELL SETUP	25
DEVICE DESIGN.....	26
TREATING, OBSERVATION OF PRINTED VESSELS AND STATISTICAL ANALYSIS	27
WELL SET UP	35
CHAPTER IV. RESULTS AND DISCUSSION.....	29
CELL MORPHOLOGY AND VIABILITY.....	31
OBSERVATIONS	35
CHAPTER V. CONCLUSION	42
CHAPTER VI. RECOMMENDATIONS FOR FUTURE WORK.....	44
REFERENCES	46
BIOGRAPHICAL SKETCH.....	55

LIST OF TABLES

	Page
Table 1: DOE table; EDTA and collagen were utilized as the factors of this experiment.....	25
Table 2: 24-hour measurements. In red are failed samples. 24 hours was taken only for tubule structures.....	32
Table 3: 72-hour measurements. In red are failed samples. 72 hours was taken for both tubule structures and 3D-well setups. Included in the 72 hour live/dead assay is the presence of vWF.	32
Table 4: Graphical comparison between EDTA and nonEDTA treated samples at 0.40% and 025% collagen content at 24 hours.	34
Table 5: Graphical comparison between EDTA and nonEDTA treated samples at 0.40% and 025% collagen content at 72 hours.	34

LIST OF FIGURES

	Page
Figure 1: Steps of the biomanufacturing process.....	5
Figure 2: Coaxial setup with 2 syringe pumps and x, y, z stage.....	24
Figure 3: Pattern for printed structures	25
Figure 4: CAD model of device, rendered	26
Figure 5: Stabilized extrusion left, unstable right.....	29
Figure 6: Collagen-alginate hybrid structures phenotype, and scaling. Top left: 1593.97 um. Bottom center: left wall 169um and left wall 211.05 um. Blue color is from blue-dyed CaCl ₂ solution to track solution location during printing and perfusion in tubules. Blue often spread to the rest of the structure due to diffusion.....	30
Figure 7: Cultured HAECs in culturing dish with maximum confluency. Two images are shown, both of the same passage and line, to show different plates and the various elongation and morphological patterns taken by cultured HAECs.	31
Figure 8: vWF presence in 0.25 nonEDTA treated, a-c were fluorescent view and d was not.....	33
Figure 9: a) EDTA treated 0.40% collagen, b) non-EDTA treated 0.40% collagen, c) EDTA treated 0.25% collagen, and d) non-EDTA treated 0.25% collagen at 24-hour initial incubation without added cells.....	35
Figure 10: a) Color image of 0.4 EDTA treated and b) Live (green) of lower level of 0.4 EDTA treated tubule. Paths are inside to outside.	36

Figure 11: Both images are of the 0.4 non-EDTA treated structure in different areas. Circled in white are examples of cell-lead paths. Paths are outside to inside.36

Figure 12: Viability Live(green) 0.25 nonEDTA treated.....37

Figure 13: Viability live(green) 0.25 nonEDTA treated.....38

Figure 14: Viability live(green) 0.25% nonEDTA treated. Bottom to top focus progression part 1. Top left is the bottom of the plate (L to R).....38

Figure 15: Bottom to top progression part 2; left to right. Bottom right image is the very top of the structure.39

Figure 16: 0.25% live(green) EDTA treated. Border of tubule structure and attached cells at the of the plate.39

Figure 17: Cell at the end of a migration path. Notable lattice structure left behind.....40

Figure 18: Example of swelling behavior and 4X view of tubule structures in comparison to original 14 gauge needle (2.11mm outer diameter).....41

CHAPTER I

INTRODUCTION

Additive Manufacturing

Additive manufacturing or 3d printing is a branch of manufacturing that specializes in additive construction of parts, prototypes, and finished products. Additive Manufacturing (AM) encompasses strategies that allow for rapid prototyping and finished products (Gibson, Rosen et al. 2015). These processes include both traditional and novel printing processes that fall under these categories: vat photopolymerization (VP), powder bed fusion (PBF), material extrusion (ME), material jetting (MJ), binder jetting (BJ), sheet lamination, and directed energy deposition (DED) (Gibson, Rosen et al. 2015). Prototyping involves computer-aided design (CAD) in which was analyzed via software, divided into multiple linear sections that are printed layer by layer and form the prototype (Gibson et al., 2015). Essentially, 3D printing allows for the quick translation of digital data to a physical model (Roopavath & Kalaskar, 2017).

Additive manufacturing has advanced into the medical and biotechnological fields. This form of additive manufacturing, aka 3D printing, is called 3D bioprinting. Bioprinting encompasses an extreme range of printing technologies that can fall under categories of the original base technology. 3D bioprinting includes inkjet printing, extrusion printing, laser-assisted printing, and stereolithography (Huang et al., 2017). The process itself is like any other

3D printing process with a pre-processing step that involves the translation of MRI and CAT scanned imagery to usable CAD models for printer software (Bishop et al., 2017; Williams & Hoying, 2015). These models are then used as a guide to print cells in a 3D orientation to which they can interact within hydrogels and protein or PEG-based scaffolds in which they migrate and proliferate at their leisure. In doing so, this process takes advantage of multiple different cell-behaviors in order to allow for alignment and interaction between cells dependent on aggregation and migration (Hong et al., 2013). The post-processing portion of this process involves the maturation and analysis of cells post-printing stage. Even with varying processes, the basic of 3D bioprinting is the same. This AM process uses live cells and a variety of different cell culturing, biochemical, and engineering materials by adding the same or different materials layer by layer in the hopes of creating 3D structures in which can mimic and eventually replace damaged tissues or perform as physiological specimens for clinical studies (Witowski et al., 2018).

3D Bioprinting

3D Bioprinting (3DBP) that deals with the manufacturing and processes involved with generating engineered tissues (Ong et al., 2018; Skardal, 2015; Sundaramurthi et al., 2016; Williams & Hoying, 2015). 3DBP focuses on the use of cells, biomaterials, engineering materials, and engineered processes to construct tissues layer by layer accurately and precisely. Because of this, 3DBP has shown great promise with many successful prints containing viable cells and structure. 3D bioprinting uses live cells and a variety of different cell-culturing, biochemical, biomechanical, and engineering materials. In order to form biomimetic tissues, this process utilizes the innate abilities of cells to migrate, aggregate, and communicate with one another (Hong et al., 2013). 3D Bioprinting has a requirement of understanding the mechanics of

cell behavior. With this, the possibilities of forming tissues and organs becomes a possibility. The main goal of 3D bioprinting is establishing a way(s) to print large scale and viable tissues or organs for study and replacement, essentially taking 3DBP to the clinical level (Huang et al., 2017). 3DBP has shown great promise in producing organoids and tissues (Huang et al., 2017; Kengla et al., 2015; Zhang, Yue, et al., 2017). Currently, bioprinting has been involved with a number of different tissues such as bone (Keriquel et al., 2017; Park et al., 2014), cartilage (Roseti et al., 2018), vessels (Hoch et al., 2014), cardiac tissue (Ong et al., 2018), muscle (J. H. Kim et al., 2018), skin (Tarassoli et al., 2018) and even neurons (Huang et al., 2017). However, even with progress on maintaining viability within and after the printing process, prints are limited to small statures and thin thicknesses due to the lack of usable vasculature.

3D Bioprinting and Vasculature

Vasculature is a primal and important system for tissue communication, nutrient delivery, oxygen provision, waste removal, and the capability of stature in organisms. This network of vessels connects and allow for the interaction between cells and tissue structures on the chemical level via juxtracrine, paracrine, and endocrine pathways. Within biological boundaries, the first system established for embryonic development is a connection to an established vasculature. Within the constructs of vasculature, the basic cells required for forming capillary systems are endothelial cells. These cells will exhibit morphology which changes the physical properties of the capillary that will in turn affect the permeability of capillary systems (Sawdon & Kirkman, 2020). Endothelial cells alter their basement membranes and overall shape to create continuous, fenestrated, or sinusoidal capillaries. Each system specializes in ensuring the proper amount of

nutrients and oxygen while removing waste is occurring. Capillaries can be considered responsible for the viability of a print during and after manufacturing.

It is well established that in order to advance 3D Bioprinting to manufacture solid and functioning organs is to have an established and maintained vasculature (Jia et. al. 2016). There are many methods and processes being developed and studied for the establishment of vasculature to coexist and be present as the tissue or organ is printed. To be able to increase the thickness and size of prints, and engineered tissues, establishing vasculature is currently still a major limiting factor on the capabilities of printed tissues (Datta et. al. 2017, Zhu et. al. 2017, Ozbolat and Yu 2013). Current successful prints include the formation of lumens, co-printing benefits, pattern alignment, and in some perfusion tests for mechanical properties (Q. Gao et al., 2015; Guillemot et al., 2010; Jia et al., 2016; Kawecki et al., 2018; Kerouredan, Bourget, et al., 2019; Kerouredan, Hakobyan, et al., 2019; Xu et al., 2013; Zhang et al., 2013; Zhang, Pi, et al., 2017). Printing viable vasculature is available with some capable of being perfused and some prints capable of integrating and surviving in vivo. How can this vasculature be utilized in a printed structure?

Perhaps, if printed structures are given a point of reference, such as an established vasculature that can be then built off of, similar to what is occurring in in vivo implants but in vitro, the printed structures will have better cellular interaction as well as a decreased time frame in which the cells migrate or interact with each other all while utilizing a printing technology of choice.

Approaching the Incorporation of Vasculature

Vascularization is extremely important to maintaining and supporting sizable prints. It is not a new concept to know that vascularization will aid in the survival and maintenance of prints or engineered tissues as a vascular system is required for survival in respiring organisms. Despite this being very biological in nature, this is and will be considered a manufacturing process. The figure shown below approximates all the stages and requirements to generate functioning tissues while maintaining the integrity of a manufacturing process meant for mass production.

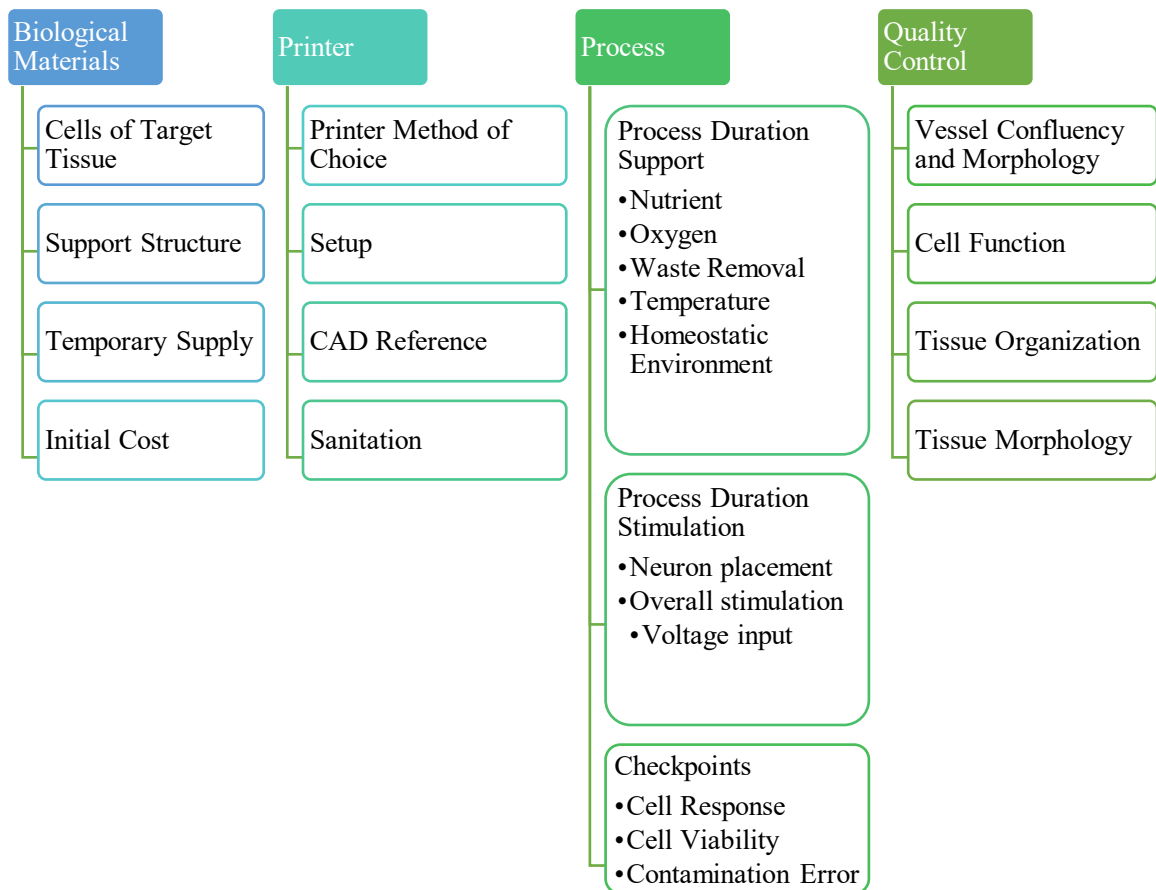


Figure 1: Steps of the biomanufacturing process

The flow chart depicted is a proposed incorporation of resources, printer setup, setup, and quality control in the bioprinting process. How can researchers incorporate printed perfusable vasculature into a 3DBP process? With the incorporation of vasculature via whatever method or approach, having vasculature within the print as it prints would inevitably streamline the AM processes.

It is hypothesized that via a device or method that provides for a preliminary established vasculature that will allow for both access to the tissue construct via the device as well as access to a biophysical and biochemical input greatly needed for vessel formation and tissue establishment. It is from this proposed approach that there is a possibility of generating a broad bed of capillaries in the future. Larger and thicker tissues will require longer periods of time in a printing environment that will end up requiring maturation and incubation environments.

What are the morphologies and interactions between coaxially printed tubules and cultured cell populations? This research involves preliminary investigations to design/improve a novel device to provide laminar flow and nutrients for possible future works in streamlining the bioprinting process and perhaps aid in the generation of capillary beds for 3D thick tissues by enabling parallel-built vessels that can allow for later vessel formation and alignment. This thesis includes the replication of known bioprinting methods to print tubule structures in order to test a modification to the bioprinting process. The modification involves the use of collagen in alginate tubules and the possibility of using EDTA to increase the porosity of the tubule structures.

CHAPTER II

REVIEW OF LITERATURE

In determining an approach to establish a preliminary vessel to be used as both a link between support system and biological system and as well as the initial ‘parental’ vessel for proximal and physical reference for later printed cell populations, the basics in vascular formation, structure, and generation was looked into as well as current vessel prints for starting points and reference.

Vasculature

Vascular bundles are of great importance in maintaining environments of organs and cells. They ensure the proper amount of oxygen and nutrient supply while keeping up waste removal. Vessels act as paths for communication from far away sources as well as nearby via the endocrine system. Vasculature allows for the establishment of an oxygen source to allow for proliferative behaviors and higher functions of tissues leading to organ development. Vasculature is essential for creating 3D structures to potentially mimic and replace damaged tissues or to be used to perform physiological testing of specimens for preclinical studies. In a clinical or laboratory setting, vasculature would act as an active conduit to exchange wastes and nutrients of in vitro manufactured tissues. This would sustain and allow longevity of structures and a point of access for pharmaceutical infusing or application. Vasculature is a primal and important system

in organisms for tissue communication, nutrient delivery, oxygen provision, waste removal, and the capability of stature in organisms. This network of vessels connects and allows for the interaction between cells and tissue structures on the chemical level via juxtacrine, paracrine, and endocrine pathways. Establishing vasculature, the initial process is done via vasculogenesis in developmental biology (Kaully et. al., 2009). Vasculature is a branching pathway that loops through various main structures: arteries, arterioles, capillaries, venules, and veins. Arteries and veins are thick muscular structures that include elastic layers of connective tissues, arteries more than veins, contain smooth muscle and endothelial cells. Arterioles and venules are a step downwards while still containing smooth muscle and endothelial cells. The smallest and by far most important in exchange, are capillaries. Capillaries vary in width and composition according to the organ they are supporting. There are continuous, sinusoidal, and fenestrated capillaries. These types will greatly determine the rate of exchange that occurs as well as what is exchanged. Capillaries and venules are commonly supported by pericytes, which are embedded into the basement membranes of these structures (Birbrair et. al., 2015). These cells perform functions of supporting structures, communication between neighboring cells, homeostasis, and wound based angiogenesis (Birbrair et al., 2015).

3D BP purposes include mimicking this initial step, vasculogenesis, using angioblastic cells or via concentrated introduction of endothelial cells. Bioprinting takes advantage of what cells are pre-programmed to do, hence utilizing cell behavior to its advantage (Hoch, Tovar, & Borchers, 2014). However, printed structures do not have established vasculature to access and utilize for the maintenance of tissues and the construction of mature cellular matrices. It is well established that in order to advance 3D BP to manufacture solid and functioning organs is to have an established and maintained vasculature. Vasculature in printed structures can be

considered the bottleneck of biomanufacturing processes. There are many methods and processes being developed and studied for the establishment of vasculature to coexist and be present as the tissue or organ is printed. Though much research is being conducted, the ability to increase the thickness, size of prints, and engineered tissues by an established vasculature is currently still a major limiting factor on the capabilities of printed tissues (Datta, Ayan, & Ozbolat, 2017; Jia et al., 2016; Ozbolat & Yu, 2013; Zhu et al., 2017). Essentially anything thicker than $\sim 200\mu\text{m}$ (Kawecki et. al. 2018), due to the lack of able vasculature, these include grafts, thick tissues, and other printed structures are incapable of being sustained in vitro or easily fused to an in vivo tissue with transplantation (Datta et al., 2017). Many prints and tissues are extremely limited to the permeability of oxygen and nutrients, approximately $100 - 200\mu\text{m}$ (Ong et al., 2018) (Ong et al., 2018; Zhu et al., 2017), as diffusion is inefficient and insufficient way to oxygenate tissues when at a sizable stature.

Vessels

Blood vessels are complex and dynamic structures that respond to a variety of inputs to maintain their physiology. In order to print a vessel, one must understand the layers in which a vessel is organized. The order in which vessels are organized from inner to outer layers is the lumen, endothelial cells, smooth muscle cells or pericytes depending on the class of vessels, an interstitial matrix with fibroblasts, and epithelial cells. In the case of 3D printing vessels, the most popular way in which to generate these is via the use of coaxial printing in which layers everything in one go. The maximum layer count can be achieved via a triaxial setup (Attalla et al., 2018).

Capillaries

Capillaries are essential to the vascular system as they are responsible for the majority of exchange. This exchange is limited to a certain portion of the capillary that will vary exchange rate via physical structure. The first and most common capillary type is the continuous capillary. This structure is the least permeable with complete basal lamina and endothelial construction with pericyte interaction. The 2nd is fenestrated capillaries also with complete construction only far less pericytes interaction and designated gaps between cells that act as pores, hence the name fenestrated. The last is the most permeable with its incomplete basal lamina and sparse endothelial cells with large windows to organ tissue called sinusoidal or discontinuous capillaries. Capillary form is directly related to the function of the capillary as it determines permeability and rate of exchange (Sawdon & Kirkman, 2020). Endothelial cells alter their basement membranes and overall shape to create continuous, fenestrated, or sinusoidal (discontinuous) capillaries. Each type specializes in ensuring proper amounts of permeability is achieved, yet still allowing access to tissues or lumens. There is such a difference in exchange that the capillary types will vary organ to organ based on the needs and responsibilities of that organ. The retina for example uses fenestrated capillaries on the choroid side and continuous on the other. Capillaries also have different flow rates within them with the choroid flow up to 150mm/s and the internal retinal flow 25mm/s. Capillaries are made up of endothelial cells in most portions. Capillaries can also have support cells called pericytes that aid in vessel health and homeostasis. Endothelial cells populate the entirety of the vessel wall.

Many prints and tissues are extremely limited to the permeability of oxygen and nutrients, approximately 100 - 200 μ m (Ong et al., 2018; Zhu et al., 2017), as diffusion is inefficient and insufficient way to oxygenate tissues when at a sizable stature. However,

diffusion is limited to a small portion of capillary beds (Sawdon & Kirkman, 2020). However, whatever the type of capillary, having some sort of starting point for printing tissues would in theory aid in the organization and support of printed cells.

Angiogenesis and Vasculogenesis

It is known that cells need inputs to generate the proper outputs in order to adapt to changing environments. ECM is a dynamic matrix working with blood vessel cells i.e. fibroblasts, smooth muscle cells, and endothelial cells in order to stabilize vessel structures and enable lumen formation in both in vivo and in vitro settings (Rajan et al., 2020). The first version of vessel generation is angiogenesis. Angiogenesis begins as a hormonal fluctuation that indicates hypoxia or a lack of oxygen. There are multiple hormones that trigger angiogenesis from hypoxia however the most prominently known one is HIF-1 (hypoxia-inducible factor) and VEGF (vascular endothelial growth factor). Commonly from injuries, when oxygen becomes more in demand, endothelial cells are triggered and over time progressively invade tissues. Maintaining a proper balance between angiogenic factors and inhibitory angiogenic factors is important in supporting tissue health and growth.

Vasculogenesis utilizes stem cells in embryonic development to generate vessels.

Bioink Properties

The main purposes of bioinks are protecting, nutrition provision, and supporting cells while the print occurs. Bioink within the scope of both printing and sustaining must have a balance in which provides the best printing parameters, and the best support and protection for cells; note that cells will/should take priority. Bioinks can be purely structural or cell laden.

Bioinks that are mainly structurally focused are designed to resist gravity and collapse to prevent the warping of printed designs. If the bioink is cell-laden, there is a need to ensure that the ink itself behaves similarly to an extracellular matrix oriented with the cells in use to provide proper mechanical, chemical, and biological means for desired morphology and function as reviewed by Browning et. al. (Browning et al., 2014).

Bioinks have to balance between structurally compatible and degradable to make way for cell-based reconstruction (Hoying & Williams, 2015; Jose et al., 2016; Williams & Hoying, 2015). It is because of this that providing cell to cell communication is essential. Some experiments have added ECM to their bioink formulations. ECM or extracellular matrix is pertinent and directly correlated to the health and function of tissues or cells and can alter the overall behavior of cells (Fernandez-Godino et al., 2018; Gillies & Lieber, 2011; Ji et al., 2018). ECM is a vital complex of fluid and protein for proper cellular function, homeostasis, and morphology (Frantz et al., 2010; Streuli, 1999). Experiments involving bioinks with ECM or components more similar to native tissue have been shown to display better morphology and cell to cell interaction.

In doing so, cells can have a more similar environment to that of native tissues. This would mean that the inputs will be more holistic and allow for the best chance of proper cell function and physiology.

Bioprinting Materials

Cells: Investigations involving endothelial cells will commonly analyze structures for lumen formation or alignment to scaffold conduit as it is a key structure that will demonstrate proper cell morphology (Kerouredan, Bourget, et al., 2019; Maiullari et al., 2018; Wu &

Ringeisen, 2010). Of these experiments, one can observe the use of co-printed cells. Wu et. al. focuses on the use of laser-assisted bioprinting for the development of HUVECs and HUVSMCs. Utilizing other cell types known for their proximity to capillaries and their innate function to regulate endothelial proliferation called co-culturing or in this case co-printing has been proven (Hong et al., 2013; Kerouredan, Bourget, et al., 2019; Wu & Ringeisen, 2010) and reviewed (Kaully et al., 2009; Sarker et al., 2018) to be beneficial in the overall result of bioprinting. Co-printing takes advantage of what is proven in cell culturing investigations such as this one and others such as these. Co-printing, though already used in some setups, should consider what is being done currently and what has been done in 3D cell-culturing to aid in not only enhancing the viability of the print but also determining what is necessary for post-processing maturation. It behooves 3DBP to utilize co-printing more often as it produces sounder results. Native blood vessels interact with a variety of cells that maintain and support them. At the larger scales, elastin layers, smooth muscle, and fibroblasts in surrounding ECM contribute to the health and physiology of blood vessels. At the smaller scale, pericytes support capillaries and interact with fibroblasts.

Internal Scaffolding and Patterns: Previous studies have shown essential abilities of structural materials for bioinks to permit the binding of cells and behave as an internal scaffold for migration of cells; for reviewed different types of scaffold designs used in 3D printing (Giannitelli, Accoto, Trombetta, & Rainer, 2014). For vasculature one of the most common structural components is collagen, more specifically collagen I, for its interactable structure and crosslinking abilities. Collagen I is the most predominantly used material for structural components in bioinks. Among other collagen types, collagen I undergo what is known as “fibrillar collagen formation” in which during optimum pH and temperatures, collagen I will

form gels (Williams et. al., 2015). Collagen is one of the most common structural proteins found in the body that aids in cell migration, proliferation, and morphology as it behaves like internal scaffolding. However useful collagen I is for structural components, collagen IV has more influence on endothelial cells and the outcome of their behavior. Collagen IV stimulates endothelial cells into forming lumens (Williams et. al.,2015). Similarly, in 3D cell culturing A review has been done on scaffold types considering the same concerns (Knight & Przyborski, 2015). However, for the ease of handling in a lab setting, the pepsin solubilized collagen was chosen for its gelling properties at room temperature and higher versus acid prepared collagens which begin gelling at far lower temperatures.

Among other experiments, proximity is necessary to ensure cell alignment parallel to the lumen or flow (prints that mention alignment via printed structure). A determinant of cell abilities within a bioink scaffolding is cell proximity to structures. While this can be avoided with cell-laden bioinks, some instances require a different type of bioink for strictly support or barrier properties. An example of scaffold prints utilizing proximity include Maiullari et. al.'s (Maiullari et. al., 2018) experiment that involved myocytes and HUVECs. The introduction of endothelial cells within their varying scaffold patterns of 2:2:2:2:2, 4:2:4, and Janus showed the importance of proximity of cell types in a 3D orientation. Janus proved the better option for endothelial lumen formation and that the endothelial portions remained confined to the printed fibers.

Oftentimes, bioprinting experiments involve patterns to create the A patterned print is any process that intends to imitate the shape of a vessel. Coaxial printing is by far one of the most popular to do this as the axial nozzles allow for an immediate layering of structural and cell-laden materials. Extrusion prints do the same thing only with having to create the pattern via

separate lines of ink. An example of patterned printing would be Gao et. al.'s (Gao et. al., 2015) coaxial setup.

Whether the use of strictly structure or pattern-based approaches, the components that support the gel are extremely necessary for the integrity of a print and for the ability of cells to cling and utilize the structure for migration and adhesion.

Another way this can be approached is using more than one type of gelling material (Correa et al., 2020; Jia et al., 2016; Maiullari et al., 2018). These dual material hydrogels involve the dissolving of one and the maintaining of the other. Of the combinations of hydrogels, calcium-alginate gels with collagen gels seems the more promising, enabling for pure collagen structures without the inhibition of alginate gels via the use of EDTA or sodium citrate.

Mechanical Strength: In some investigations, tests on solidified structures for mechanical strength were done as a precursor to perfusion (Jia et al., 2016; Zhang et al., 2015). These structures were then built cell laden. In doing so, these perfusions also tested shear stress reactions much like Nguyen et. al. Via the use of a TPS bioreactor, hMSCs, and ECs were co-cultured and the scaffold materials of alginate and collagen were examined (Nguyen et. al., 2017). This investigation concluded that proximity was a must as well as collagen being the preferred scaffolding for its binding capabilities. The use of TPS bioreactor also demonstrated the cooperation of the co-cultured cells and shear stress. In Jia et. al., cells within the vessel construct reached confluence and thus imitating natural vessels. Testing perfusion also tests for the quality of the vessel manufactured.

The basic mechanics of bioink involves a multitude of parameters to combat shrinkage, shear stress, collapse, and degradation. Often times collagens and CaCl₂ infused alginates prove

to be structurally sound with the ability to withstand flows, demonstrated via coaxial experiments (Q. Gao et al., 2015; Jia et al., 2016; Zhang, Pi, et al., 2017).

Bioactive Components: Another part of bioinks that hold considerable power in determining cell morphology and behavior is bioactive components. Content within bioinks include: an energy source known as glucose, amino acids, vitamins, a pH buffer, and a salt solution. ECM is extremely crucial in the native environments of tissues because not only is it used for support, it is also used for biochemical and biomechanical cues for proper morphogenesis, differentiation, and homeostasis (Frantz, Stewart, & Weaver, 2010). ECM affects binding and cytoskeleton mechanics which in turn contribute to the overall morphology and function (Browning et al., 2014; Wang & Ingber, 1994). Several bioinks have used ECM components or ECM itself to contribute to print outcome (Hong et al., 2013; B. S. Kim et al., 2018; J. Kim et al., 2019; Li et al., 2018; Shafiee, Norotte, & Ghadiri, 2017; Skardal, 2018). Some experiments are using decellularized extracellular matrix (dECM) to include into bioinks or hydrogels (Dorgau et al., 2019; Frenguelli et al., 2018; Janson & Putnam, 2015). Within ECM, a multitude of proteins and hormones that interact with the cells it is in proximity to. In the case of endothelial cells or vessel structures, cells that interact with ECs and ECM interstitial space will release homeostatic factors and regulatory factors for vessel formation and homeostasis. Some factors that are pro-angiogenic factors include VEGF, FGF, recently discovered effects of T4 and T3, and anti-angiogenic factors TSP-1 (Bridoux et al., 2012).

The use of bioactive materials will allow for better imitation of living systems, as done and investigated with multiple experiments. It will aid the biomanufacturing process to involve input such as these to align and solidify prints.

3D Bioprinting Processes and Tubules

Experiments reviewed were selected via processes involving any endothelial cell line, lumen patterns, lumen formation, conduits, and microtubules directed towards the pre-vascularization or vascularization of printed tissues. Depending on the printing process used will determine the viability outcome, cost, time, risks, and precision (Bishop et al., 2017). Extrusion bioprinting involves the use of various forces which cause the extrusion of bioink or biomaterials onto a receiving surface or plate via nozzle. This process can utilize pneumatic, piezoelectric, or mechanical forces. These printers, though much easier to handle and set up at a cheaper cost, involve forces that can harm or damage cells. However, in recent advances, stress and harm to the cells have been minimized. Laser printers, laser-induced forward transfer (LIFT) or laser-assisted bioprinter (LAB). LABs are commonly used for their low cell stress and low mortality rates (Kerouedan, Bourget, et al., 2019). These printers are known for their precision and high resolution as well as their ability to handle multiple phases of matter (liquid or solid) and high viscosity bioinks (Dababneh & Ozbolat, 2014; Derakhshanfar et al., 2018). These printers involve the use of a laser that is focused through various lenses into an absorbing layer, commonly metal such as gold, that interacts with the bioink (Kerouedan, Bourget, et al., 2019; Ong et al., 2018). This laser causes a jet or droplet to form in the bioink that is expelled and is deposited onto a medium a distance below it. Despite its abilities, laser printers tend to be on the rare side as they are not only expensive to build or buy, they are also expensive to run considering the materials used. Inkjet printers are piezoelectric systems that specialize in fluid phase inks that utilize shock waves produced via quasi-adiabatic reduction to jet droplets onto a designated surface (Singh et al., 2010). Inkjet is a programmable no contact printing process that can handle multiple materials (Campbell & Weiss, 2007; Singh et al., 2010). Another printer

type is called electrohydrodynamic bioprinter or EHD. EHD printers are a new technology involving an electric field to pull material through a syringe for variable precision and accuracy. Their printing capabilities can be course with continuous jetting or drop by demand depending on the electric field applied.

Out of the many types of printers, of the investigations involving vasculature, LAB, extrusion, and inkjet make up the majority of the tested strategies. Of the few strategies in LAB focused on vessel printing, in which each of these investigations proved the capability of the printer with viability related to laser power, vessel like constructs were formed (Kawecki et al., 2018; Kerouredan, Bourget, et al., 2019; Wu & Ringeisen, 2010) and viable cells were printed (Antoshin et al., 2018; Catros et al., 2011). Dominating extrusion printers involves coaxial printer setups. Coaxial printers are most popular in creating macro vessel structures with mechanical strength and perfusable characteristics (Q. Gao et al., 2015; Jia et al., 2016; Zhang et al., 2015). More traditional extrusion prints also have been proven capable of vessel constructs (Kang et al., 2016; B. S. Kim et al., 2018; Kolesky et al., 2016; Norotte et al., 2009; Sooppan et al., 2016). Inkjet printers have capabilities in vessel structure production as well (Christensen et al., 2015; Cui & Boland, 2009; B. S. Kim et al., 2018; Kolesky et al., 2016; Xu et al., 2013). There are no experiments utilizing EHD for strictly vessel formation.

According to the literature, it is possible to print tubule structures that are purely just the structure or that are infused with cells. Choosing which printer for this experiment started out with a review of alginate bioinks for vascular tissues that concluded coaxial printers would be able to introduce hollow structures for on demand vessel tubule formation (Axpe & Oyen, 2016). As it turns out coaxial printers seemed the most promising (Q. Gao et al., 2015; Jia et al., 2016; Yu et al., 2013)

Possible Similar Technologies or Concepts

Organ on a Chip: point out the difference; though a similar output can be achieved, the goal of this thesis is to analyze the process components, hypothesize a possible method of ensuring a starter vessel for future printing integrity and in which can be used during the duration of a print once established. This will look into the cell behavior surrounding and within the printed vessel, the step after printing viable vessel structures via coaxial printing.

Overall

Even via engineering strategies, 3DBP must consider the processing of printing/tissue engineering. A growth phase, maturation phase, testing phase, and maintenance phase must be developed after an established process of developing viable and mimetic tissues is created. It is by the hierarchy of developmental biology that it is safe to assume that an established vasculature is the key to ensuring the survival of complex structures like support beams in a large complex building. Overall, the goal is to have stable vessel with cells that interact with the proximal layers that ensure homeostatic response and regulation. Bioinks must be able to gel at body temperature and be usable at room temperature.

From the literature, it can be acknowledged that grafting prints give insight to the possible setup of in vitro systems that imitate established structures. Another point to maintain while developing in vitro systems is the printed graft, albeit inserted for testing, was viable after a duration of time interacting with a living system. It begs the question that if a system imitated a living system well enough will the parameters allow for an improved printing environment (Maiullari et al., 2018).

3D printing is meant to lessen the time of cell organization by putting cells in the initial pattern. Bioprinting handles placement and with certain materials, the physical inputs for cell feedback loops involving proliferation, migration, and alignment. Bioinks can contribute to the physical, chemical, and biochemical signaling to guarantee the desired outcome. Cells are capable of self-regulation. It has already been proven in a plethora of methods that printing cells and keeping them viable is possible with cell able to migrate to a desired location. A good number of printing strategies can now produce vessel structures. Formation of viable vessels is possible, but is function possible? Experiments thus far have proven viability and have also proven capabilities of printing processes with multiple cell types and bioinks. It has also been proven that some structures are perfusable. What is this process missing to allow prints to have maintained vasculature?

There are multiple examples mentioned that allude to the ability of printed structures to survive and thrive in vivo. However, the goal of 3DBP, and any other tissue engineering mechanism, is functional tissues to thrive in vitro for the sake of studies and organ production. If this is to occur in vitro to enhance the process of biomanufacturing, for the hope of producing organs and tissues in a controlled environment for studies and therapies, a developed system to provide living stimuli via an established vessel system should aid in the polarization of cells and their ability to align to existing vessels for nutrient delivery throughout a print.

This thesis uses the 3D coaxial printing method with commonly used materials such as alginate and calcium chloride solutions to generate hollow tubules while adding a content of collagen proteins to the bioink in order to integrate a scaffold protein known to interact with endothelial cells especially with adherence using alginate as a sacrificial hydrogel in hopes to

make porous collagen tubules to interact with added cell populations to analyze cell morphology and behavior with printed tubule structures.

CHAPTER III

METHODOLOGY AND MATERIALS

Culturing Cells, and Stock Solutions

Primary human aortic endothelial cells (HAECs) from Cell Systems were prepared with Complete Classic Medium and Antibiotic-Antimycotic. Cells were removed from the cryo-storage and partially thawed. They were then resuspended in 1mL of complete media to neutralize DMSO content in the vials. Cells were then suspended in media before being centrifuged for 10 minutes at 900 rpms at 14-24C. Media was aspirated from conical containers and the cell pellets were resuspended in 1mL of prepared media before being transferred to culturing dishes.

CaCl₂ and Na-Alginate stock solutions were prepared via weight/volume. For all stock solutions of CaCl₂, milliQ (sterile, filtered water) water was used, and all alginate stock solutions, PBS 1X was used. CaCl₂ solutions (2% and 3%) vortex for 1-2 minutes. 3.2% alginate solution was prepared over-night via magnetic stirrer, and 8.2% stirred by hand with stir rod until homogenous (was stirred again after resting over-night). Alginate stock solutions were sterilized via autoclave at 121C for 20 minutes and was then stored at 4C. CaCl₂ solution was stored at room temperature.

Bioink Formulation

Bioinks was prepared with fixed 1.7% alginate and varying collagen (0.25% and 0.4%) concentrations based on previous investigations in the lab. Bioink was prepared in 6mL batches via the use of the $C_1V_1 = C_2V_2$ (done twice: once per collagen dilution then with alginate dilution) rule in order to find which alginate concentration to make to generate the proper collagen dilution from a stock 6 mg/mL (0.50%), i.e., 4.8mL of 0.5% collagen was added to 1.2mL of 8% alginate to make a 0.4% collagen, 2% alginate solution with added 6mg to adjust 1.6% to 1.7%. Bioinks were made in succession to prevent unnecessary cell death with about 8 million cells/mL.

Printer & Well Setup

Two syringe pumps were setup next to one another in a biosafety cabinet (BSC). An x,y,z stage was setup next to the syringe pumps and connected to an in lab computer with stage movement software. The system was sterilized with 70% ethanol, and then with UV light exposure for 15 minutes. Tubing was rinsed with ethanol then with PBS 1X for the collagen/alginate tubing and CaCl_2 pf appropriate concentration before being sterilized via 70% ethanol on the outside and put into the BSC.¹

¹ Cell culturing and printing labs were located in the same building. Prints, and bioinks were transferred via sealed container.



Figure 2: Coaxial setup with 2 syringe pumps and x, y, z stage.

Printing

The wall of a brand-new vessel to be printed that can only be supported via media must remain within the range of oxygen permeability, around 150um. This means the vessel size depends on the size of the lumen or lumen generating nozzle which can be calculated by subtracting the inner diameter of the outer nozzle from the inner nozzle's inner diameter.

$$t_w = ID_o - ID_i$$

This number still includes the wall diameter of the inner nozzle. The final diameter of the hollow structure is determined by the outer nozzle as found by (Qing Gao et al., 2015). Nozzles were chosen based on the ease of flow from viscous solutions and the limitations of oxygen permeability. This experiment utilized a 1418 gauged coaxial nozzle (outer-inner gauge).

Preliminary experiments concluded with alginate percentages to be 1.7% optimum for this nozzle size as well as 2X minimum CaCl_2 solution concentration for accurate tubule wall widths and tubule formation behavior. The experiment was setup with factorial design with each setup having a duplicate.

Printing Tubules and Well Setup

		Factors		Note
		EDTA	Collagen	Alginate
*Use 2D cultured cells for control				
1	EDTA treated	0.25	Minimum	
	nonEDTA	0.25	Maximum	
	3D-well	0.25	None	
4	EDTA treated	0.4	Minimum	
	nonEDTA	0.4	Maximum	
	3D-well	0.4	None	
7	EDTA treated	0.25	Minimum	
	nonEDTA	0.25	Maximum	
	3D-well	0.25	None	
10	EDTA treated	0.4	Minimum	
	nonEDTA	0.4	Maximum	
	3D-well	0.4	None	

Table 1: DOE table; EDTA and collagen were utilized as the factors of this experiment

Tubules were printed via coaxial printer at 800uL/min for both solutions. Finalized volume and approximate length were necessary to calculate an approximate cell count within alginate walls. Due to technical difficulties and a lack of programmable stage software for patterns, the printer was allowed time to print in a culturing dish in which a simple cross/ flower-like design was patterned by hand (the plate was moved by hand not by stage).

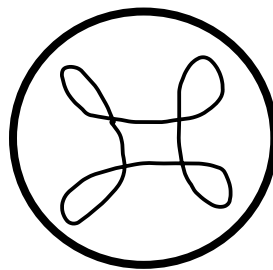


Figure 3: Pattern for printed structures

Whether or not the pattern was symmetrical or how accurate it was to the original design was beyond the scope of the design, having at least four areas in which to seed cells in higher concentrations after printing was far more important. Having these separated areas would allow for cells to be placed in certain areas to compare between cell contacted tubules and non-cell contacted tubules with internal cell population.

Device Design

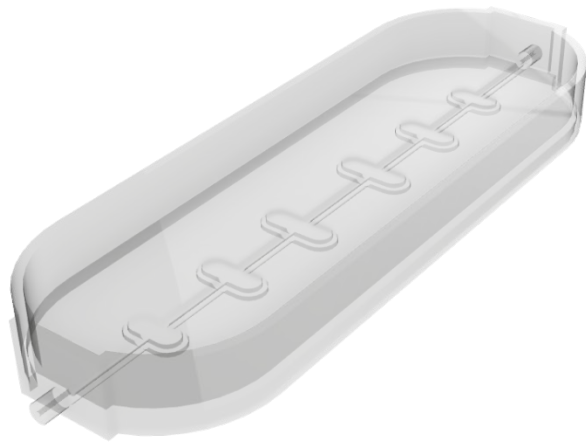


Figure 4: CAD model of device, rendered

The device was intended to have varied/ unvaried well sizes in order to track time, distance, individual populations, and gene expression separately in post printing cell cultures with coaxially printed tubules. These wells are substituted by the sectioned areas generated via tubule maneuvering. The input and output of the device is replaced by steady hands and the use of a 27- or 30-gauge needle to flush the tubule of CaCl_2 solution after printing and media after culturing cycles. The finalized device was to be clear and of appropriate size to for ease of use as well as include a lid with a raise border for easy stacking. The device would have also had a way

to seal input and output openings to guarantee sterile environments and containment of internal fluid.

Well Set Up

Wells were setup in a 6 well plate to contain appropriate concentrations of collagen content of 0.25% and 0.4%. The cells were detached from the culturing dishes and resuspended in collagen and media (diluting factor) before being put in the wells and incubated overnight. The number of cells depended on the available cell population and varied based on the dilution. Cell viability was tested at 24h and 72h with vWF tagged at 72h as well. These wells were considered “3D-well” for differentiation.

Treating, Observation of Printed Vessels and Statistical Analysis

The experiment was done twice, once with cells and once without. Tubules printed without cells were used for printer calibration, EDTA reaction, and tubule behavior in the incubator without media. Printed structures with cells were transported from the printing lab to the culturing lab in a sealed container. Tubules meant to be soaked in EDTA for 2 minutes were first incubated with media to neutralize CaCl_2 ion content for 1 hour then soaked in 2mM EDTA for 2 minutes, gently shaking, and then rinsed with media. Each fluid was vacuumed out.

Plates were incubated at optimal conditions for 24 hours and then were checked after cell addition at 24 hours and 72 hours. Wells were checked at 72 hours. Matured and solidified vessels were observed under light, confocal microscope, and fluorescence microscopy. Vessel structures were observed whole and with tags for live/dead ratio as well as vWF protein tags (Chouinard et al., 2009; Jia et al., 2016). Live/dead tagging was done following the company

protocol as well as the vWF tagging. Statistical analysis was done via 2 sample t test on MiniTab 19 with $\alpha = 0.05$.

CHAPTER IV

RESULTS AND DISCUSSION

Collagen-alginate hybrid structures were successfully printed with the novel coaxial printer setup. Collagen tubules were extruded from the system, albeit a lag time of 30 – 120s, at 800 $\mu\text{L}/\text{mL}$ for each fluid, bioink and CaCl_2 solutions. The chemical reaction stabilizes after the lag time and will continuously extrude a tubule structure. Figure 5 shows a visible difference in stabilized extrusion and non-stabilized extrusion.

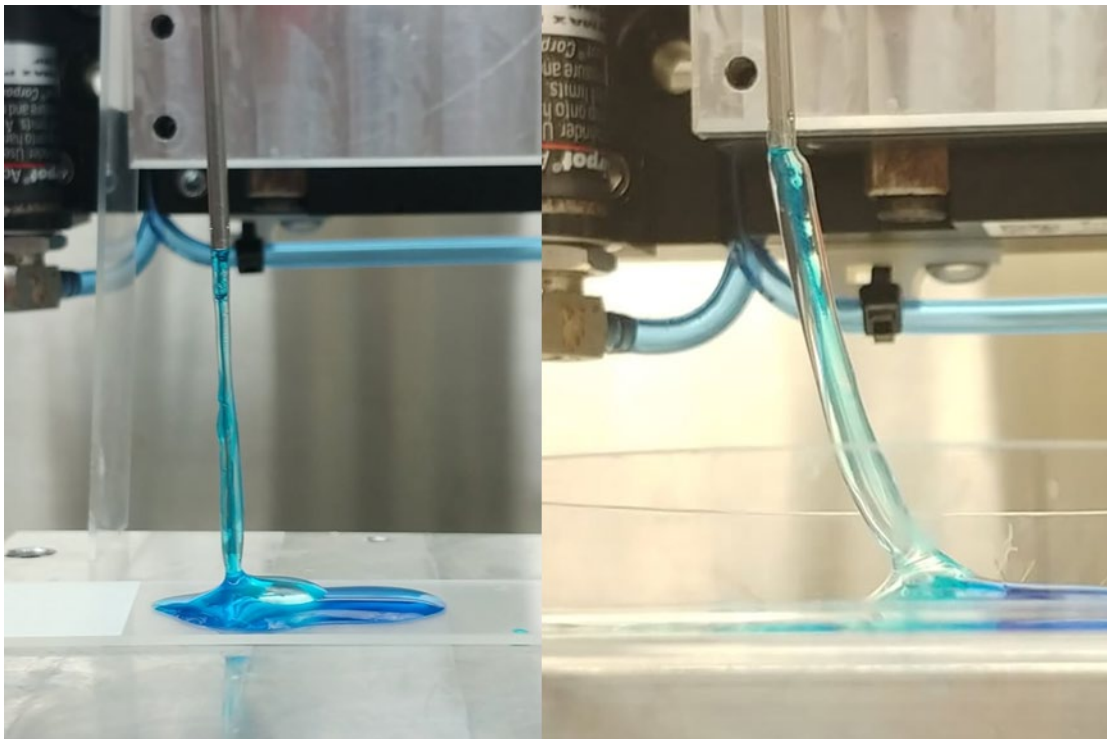


Figure 5: Stabilized extrusion left, unstable right.

Structures without cells were successfully printed and analyzed for size consistency and overall phenotype when interacting with ETDA and approach to tubule interaction. Size examples and phenotypes are shown in Figure 6. All prints and culturing setups were compared to HAECs cultured in media and allowed to become confluent over 72 hours. In order to have a proper baseline of comparison HAECs were allowed to reach 100% confluency in cell culturing plates. Plates imaged showed morphology in 2D format, and general growth patterns following the flow of cell elongation. An Excel sheet of all of the data was generated to comprehend LIVE/DEAD percentages, cell morphology scores, and vWF presence.

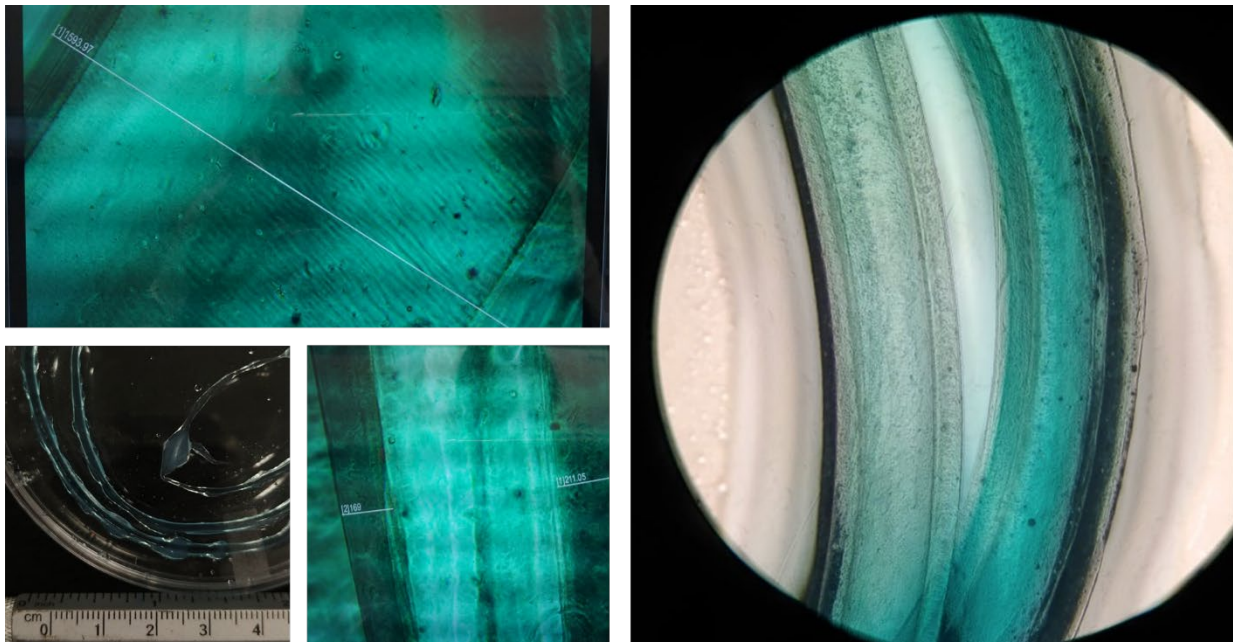


Figure 6: Collagen-alginate hybrid structures phenotype, and scaling. Top left: 1593.97 μm . Bottom center: left wall 169 μm and left wall 211.05 μm . Blue color is from blue-dyed CaCl_2 solution to track solution location during printing and perfusion in tubules. Blue often spread to the rest of the structure due to diffusion.

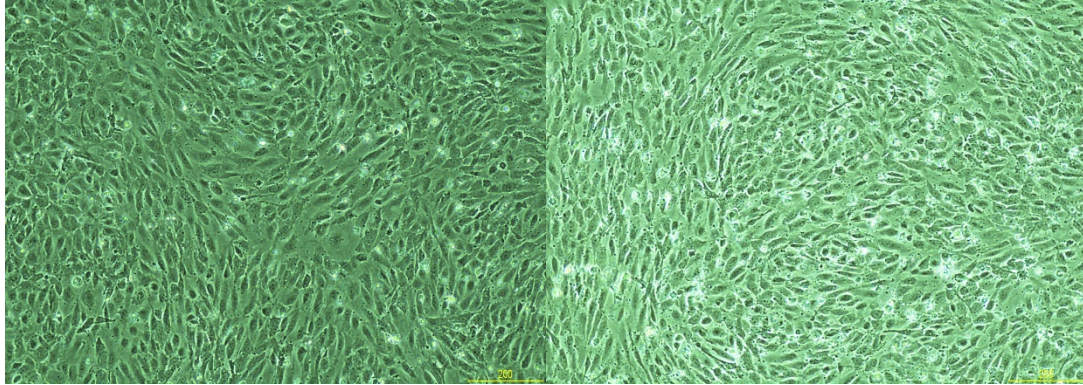


Figure 7: Cultured HAECs in culturing dish with maximum confluency. Two images are shown, both of the same passage and line, to show different plates and the various elongation and morphological patterns taken by cultured HAECs.

Cell Morphology and Viability

Both the live dead assay and the vWF stain can show morphology as well as confocal microscope. Cells attached with attachment factor around the tubule structure were captured as well as the tubule structure. Overall, with or without EDTA treatment, the cells remained in the 1 or 2 morphology score. In other words, the majority of cells within the construct remained round to oblong in shape. According to a two-sample t test, the live-dead ratio was not statistically significant between collagen percentages at 24 hours for tubule structures and at 72 hours for tubule structures and collagen gels at an $\alpha = 0.05$. EDTA treatment also proved not to be statistically significant between viabilities at 24 and 72 hours.

24h	Factors		Note	Response	
	EDTA	Collagen	Alginate	Live/Dead Assay	
	*Use 2D cultured cells for control			Live %	Dead %
1	EDTA treated	0.25	Minimum	87%	13%
2	nonEDTA	0.25	Maximum	79%	21%
3	3D-well	0.25	None		
4	EDTA treated	0.4	Minimum	83%	17%
5	nonEDTA	0.4	Maximum	80%	20%
6	3D-well	0.4	None		
7	EDTA treated	0.25	Minimum		
8	nonEDTA	0.25	Maximum		
9	3D-well	0.25	None		
10	EDTA treated	0.4	Minimum		
11	nonEDTA	0.4	Maximum		
12	3D-well	0.4	None		

Table 2: 24-hour measurements. In red are failed samples. 24 hours was taken only for tubule structures.

72h	Factors		Note	Response		
	EDTA	Collagen (%)	Alginate	Live/Dead Assay		Morphology
	*Use 2D cultured cells for control			Live %	Dead %	vWF
						T/F
1	EDTA treated	0.25	Minimum	82%	18%	1 F
2	nonEDTA	0.25	Maximum	66%	34%	2 T
3	3D-well	0.25	None	100%	0%	2 F
4	EDTA treated	0.4	Minimum	94%	6%	1 F
5	nonEDTA	0.4	Maximum	84%	16%	1 F
6	3D-well	0.4	None	100%	0%	3 F
7	EDTA treated	0.25	Minimum			
8	nonEDTA	0.25	Maximum			
9	3D-well	0.25	None	100%	0%	3 F
10	EDTA treated	0.4	Minimum			
11	nonEDTA	0.4	Maximum	70%	30%	1 F
12	3D-well	0.4	None	100%	0%	3 F

Table 3: 72-hour measurements. In red are failed samples. 72 hours was taken for both tubule structures and 3D-well setups. Included in the 72 hour live/dead assay is the presence of vWF.

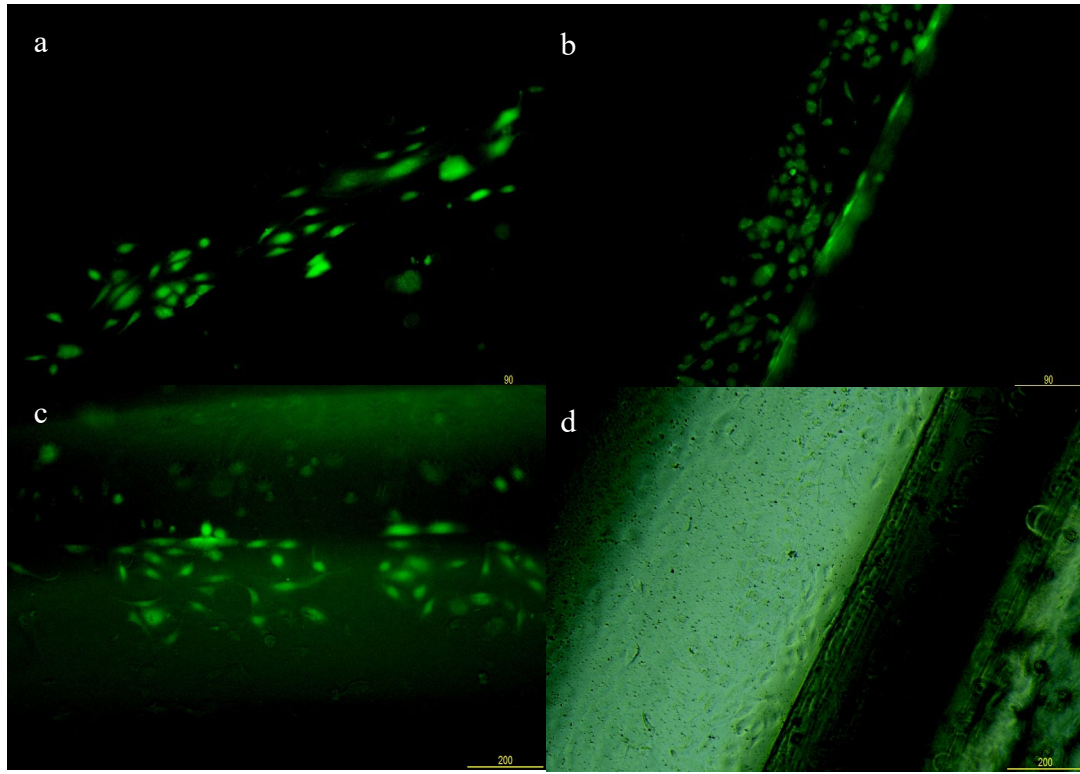


Figure 8: vWF presence in 0.25 nonEDTA treated, a-c were fluorescent view and d was not.

vWF presence in sample, shown in Figure 8, was shown via green fluorescence tag. These cells were notably aligned along the edge of the outer wall of the tubule structure with the brightest signaling belonging to that of the cells elongated along the tubule path. Comparatively, viability between 0.25% and 0.4% collagen contents was not statistically significant as well as EDTA treatment between 24 and 72 hours. Percentages are graphically compared in Table 4 and Table 5.

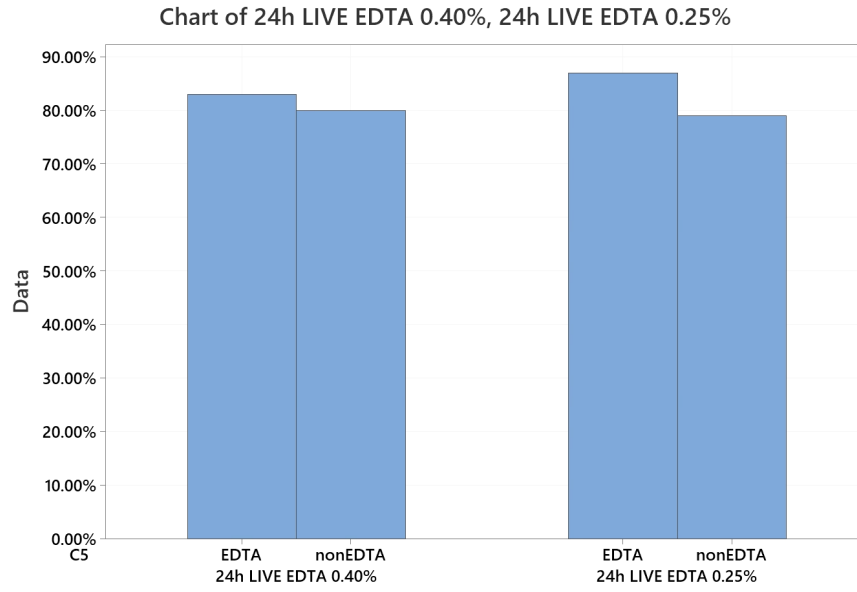


Table 4: Graphical comparison between EDTA and nonEDTA treated samples at 0.40% and 0.25% collagen content at 24 hours.

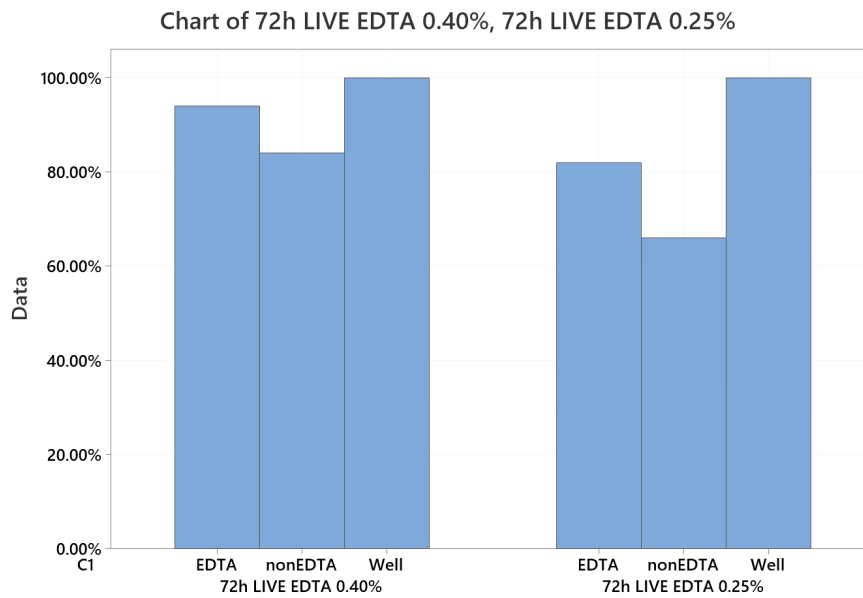


Table 5: Graphical comparison between EDTA and nonEDTA treated samples at 0.40% and 0.25% collagen content at 72 hours.

Observations

Despite careful preparation, this process involves material loss, between 1 to 2 mL, and a lag time of tubule formation that could range between 30 to 120 seconds. 0.4% collagen was more consistent with or without cells as well as maintaining its 3-dimensional shape far longer than 0.25%. Within 72 hours, 0.25% prints were deflated with a majority of cells in focus in one plane. Draining tubules without a mechanism to reseal them prevented the needed CaCl_2 solution drainage in cell prints due to the high probability of tubule collapse and deformation in media over time. Tubule dimensions remained within the same variability whether or not the structure contained cells with the lumen size varying on the speed in which the structure is laid upon the plate.

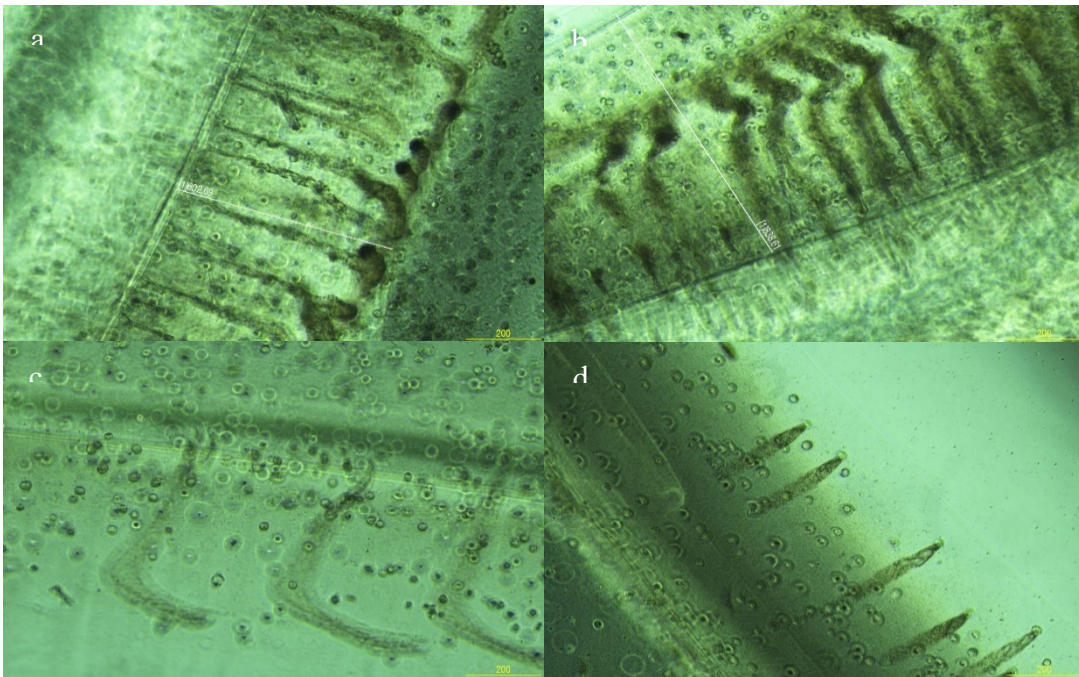


Figure 9: a) EDTA treated 0.40% collagen, b) non-EDTA treated 0.40% collagen, c) EDTA treated 0.25% collagen, and d) non-EDTA treated 0.25% collagen at 24-hour initial incubation without added cells.

Cells were shown to be able to migrate within the structure EDTA treated or not. The higher the collagen content the more paths were carved radially outward with some sort of lattice structure visibly left behind shown in Figure 9. However, in another print, 0.40 non-EDTA treated, the migration pattern was towards the center of the tubule, evident by the path ending in rounded structures, aka cells (shown in Figure 10 with still viable cells at the end points of the paths), shown in Figure 11.

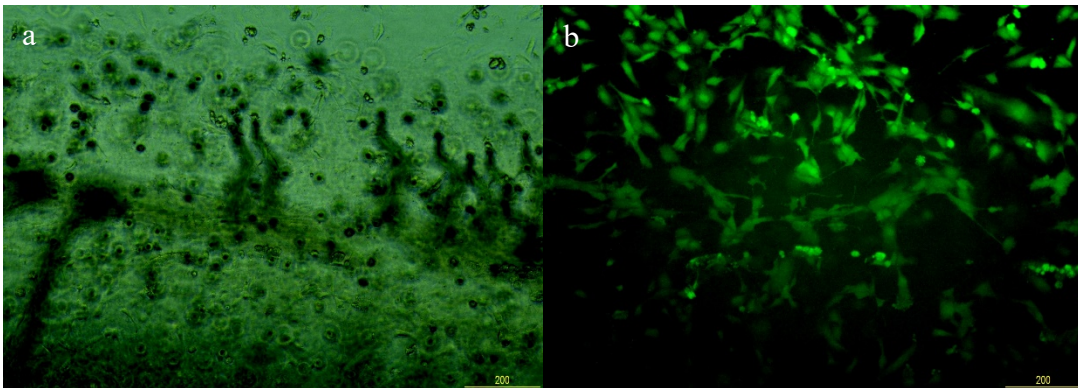


Figure 10: a) Color image of 0.4 EDTA treated and b) Live (green) of lower level of 0.4 EDTA treated tubule. Paths are inside to outside.

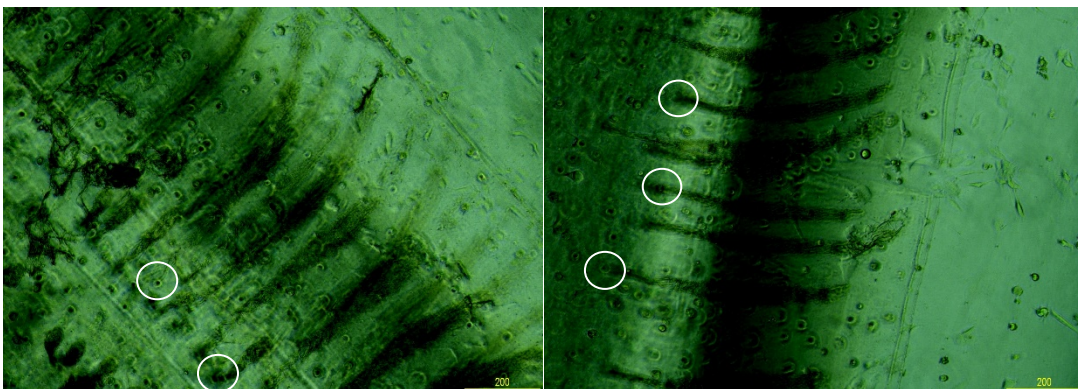


Figure 11: Both images are of the 0.4 non-EDTA treated structure in different areas. Circled in white are examples of cell-lead paths. Paths are outside to inside.

The complete opposite behavior observed in these samples gives the impression that EDTA, media, and CaCl_2 solution may affect the direction in which the cell migrate especially due to the fact that the direction was predominantly one or the other. From the images of the structures captured, it can be calculated that approximately 1-2 migration channels were formed for every 200 um^2 in the 0.25% collagen content structures and 3-4 for every 200 um^2 in 0.40% collagen structures. From this, the migration was more prominent in the 0.4% collagen. From all of these figures, 9-11, cell migration seems more prominent in higher collagen content tubules and could be directionally determined by the various treatment involved in incubation and experimentation with the paths being cell made proven by viability and microscope images.

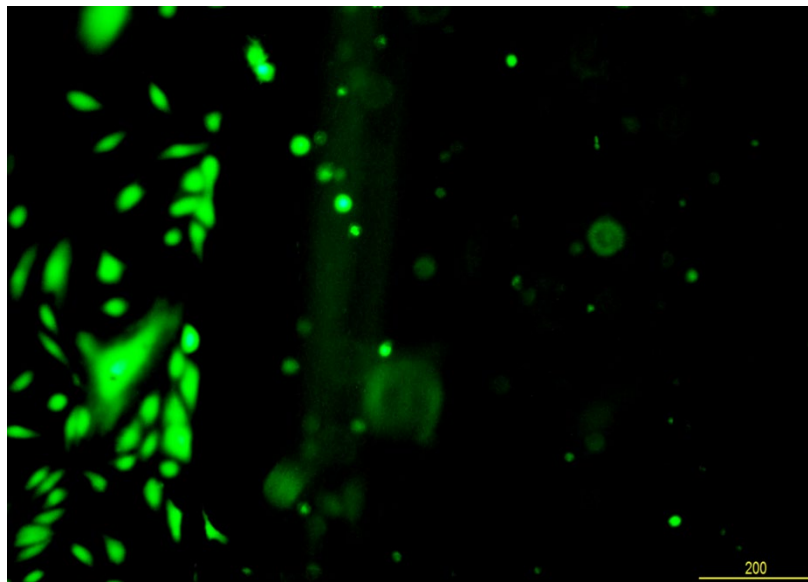


Figure 12: Viability Live(green) 0.25 nonEDTA treated

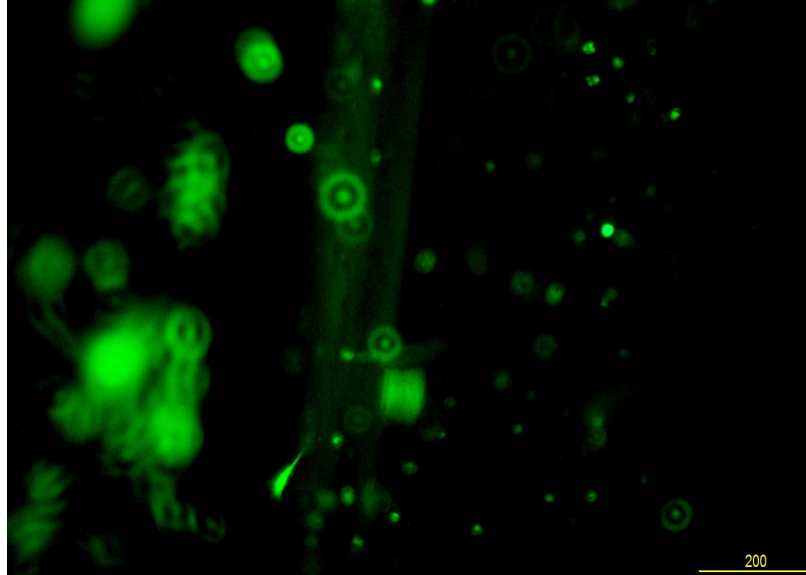


Figure 13: Viability live(green) 0.25 nonEDTA treated

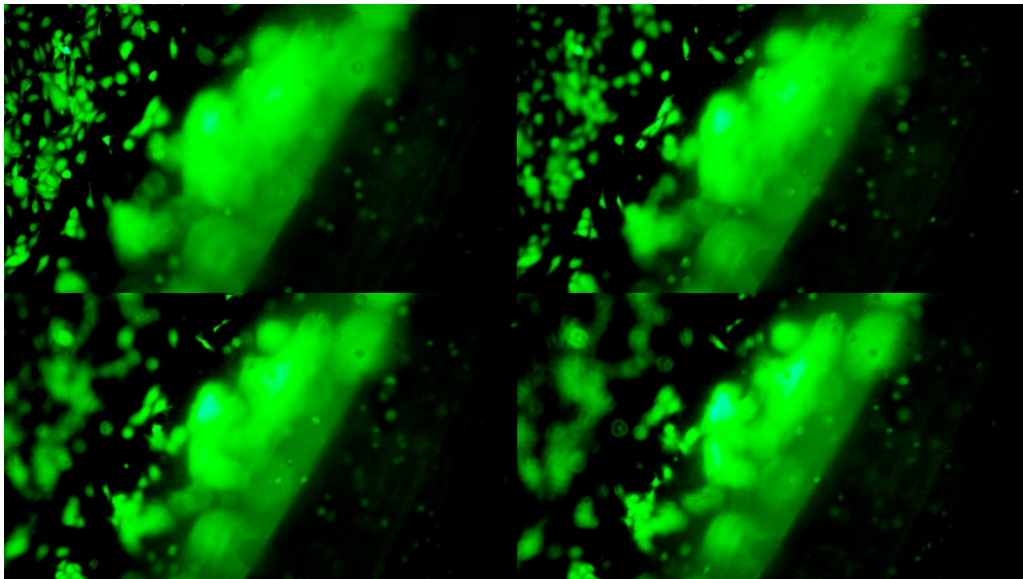


Figure 14: Viability live(green) 0.25% nonEDTA treated. Bottom to top focus progression part 1. Top left is the bottom of the plate (L to R).

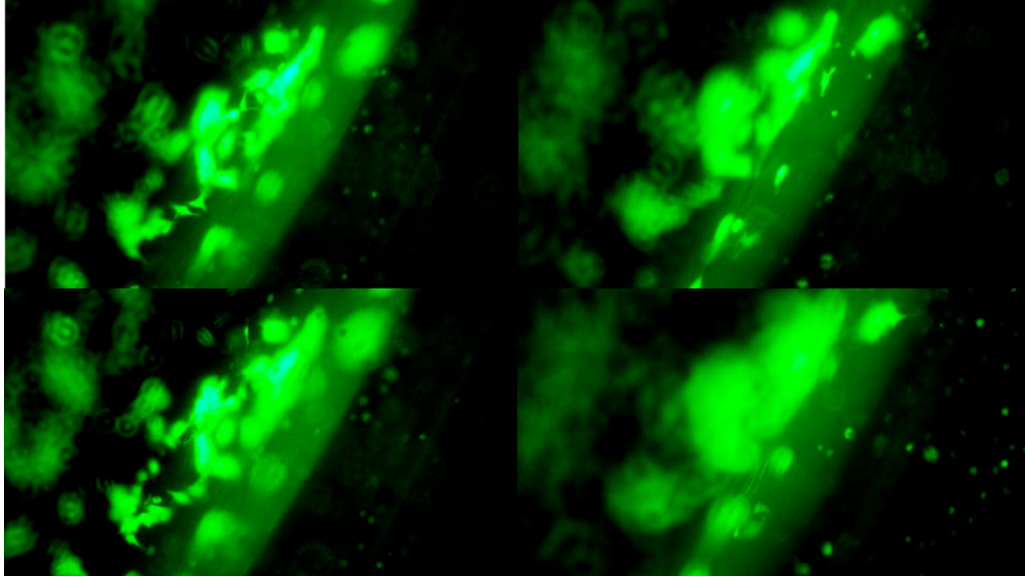


Figure 15: Bottom to top progression part 2; left to right. Bottom right image is the very top of the structure.

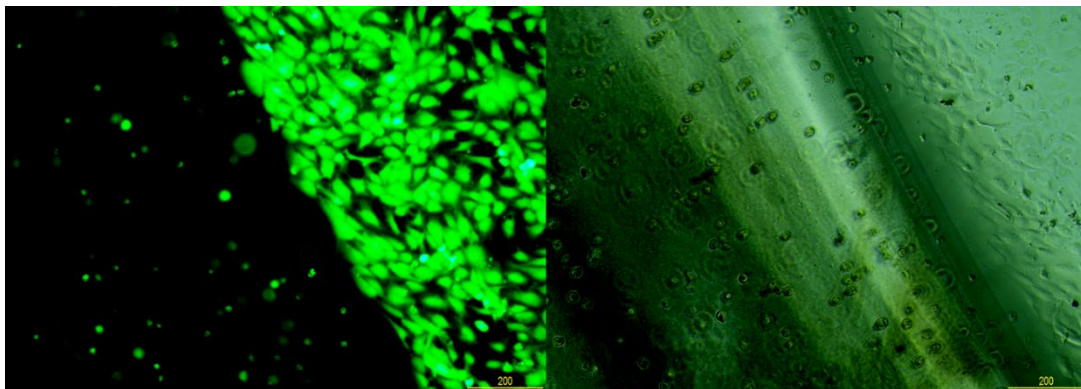


Figure 16: 0.25% live(green) EDTA treated. Border of tubule structure and attached cells at the bottom of the plate.

Figures 12 and 13, are provided to show examples of tubule structures not disturbed by the incubation process. The figures show the clear line between outer cell population and inner cell population we well as the variation between cell morphology between focusing planes. Note how

in figure 13, an elongated cell was observed at a higher (from the bottom of the plate) focusing plane. To further the differences between tubule cells and outer cells and to show the hollow status of the tubules at 72 hours, figures 14 and 15 are progressive images that, from left to right – top to bottom, show the cells in different planes of focus. The variation of cell morphologies on the outside of the tubule shows promise in the cells interacting with tubule structure to the desired degree, however, also showing the suspended cells within the tubule structure remaining more rounded in shape.

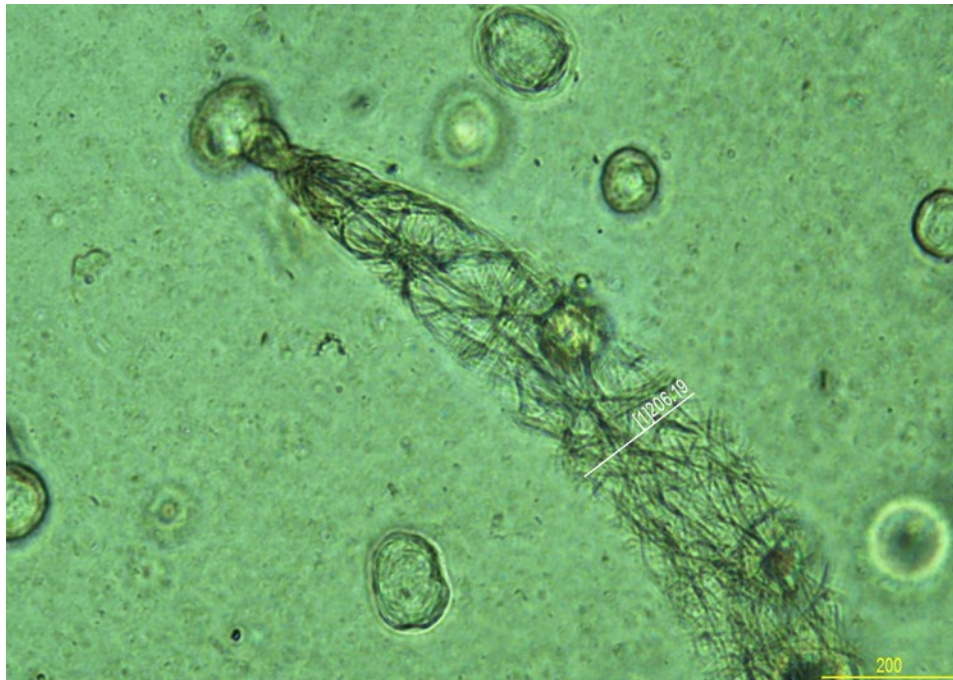


Figure 17: Cell at the end of a migration path. Notable lattice structure left behind.

To further clarify the migration of cells within printed tubule structures, figure 17 is one of many noted cell paths that left behind a curious looking structure. Also seen in figure 10 and 11, the end points were determined by the presence of a cell that some can be visually seen via live/ dead assay. The lattice seen in figure 17 was compared to crystallization structures

commonly found in test prints due to CaCl_2 presence and was not a match. The lattice appears to be either cell made or possibly collagen.

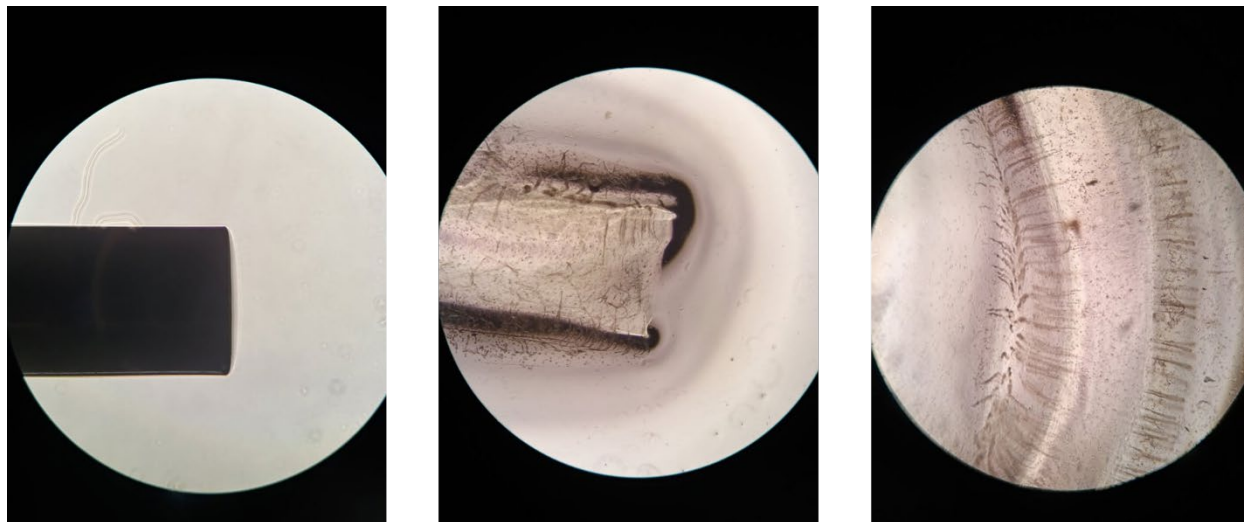


Figure 18: Example of swelling behavior and 4X view of tubule structures in comparison to original 14 gauge needle (2.11mm outer diameter)

All tubule structure were incubated for 72 hours in media. Tubule interaction with media showed that constant interaction with media caused structures to become weakened. Tubule structures showed signs of swelling noted by figure 18 with a comparison to the actual size of the coaxial nozzle used for printing. However, it is note-worthy that higher collagen content maintained the hollow-fluid filled chamber. From these observations and the behavior of the printed structures within the plates, the device designed will absolutely be necessary to maintain placement, distinct staining, lumen voiding, and protection of the tubule structure. All but one sample were detached from the plate due to movement, media changes, and perhaps even cell interaction or a lack thereof. Structures did swell to a degree and became weaker despite maintaining 3D shape.

CHAPTER V

CONCLUSION

This experiment successfully generated coaxially printed tubules via the novel setup of both the printer and bioink. Syringe pumps with combination bioink in the outer syringe and CaCl_2 in the inner nozzle at 800 $\mu\text{L}/\text{min}$ for each fluid allows for a stable enough reaction to generate tubules with collagen content. The EDTA treatment involved in the preparation of the tubules proved to be statistically insignificant concerning viability. The sodium-alginate/collagen bioink mix allows for ease of printed tubules while still being capable of interacting with cells. While the cells internal to the tubule structure maintained their round phenotype, cells against the outer walls of tubule structures were aligning themselves along the path of structure. Viability was not statistically significant between structure setups and collagen percentage. EDTA is not statistically significant effects on cell viability. vWF staining show promising use of tubule structures to align HAECs for future vessel structures for capillary beds. Higher collagen content is preferred as it maintains tubule 3D shape better and longer.

Overall, it clear that a mechanism or device is needed to maintain tubules and prevent tubule deformation. Device must include methods to ensure minimal interference, allow for the necessary internal fluid exchange, differentiating wells for different stains, and prevention of

structure movement. Structures did exhibit swelling and increasing fragility over time due to exposure to media during the incubation process.

CHAPTER VI

RECOMMENDATIONS FOR FUTURE WORK

The contributions done from this thesis will allow for the printing of collagen-based tubules for the use in tissue engineering. The process itself may improve if some of the following recommended future adjustments and studies were to be done.

The methods used in this thesis may be able to ensure pure collagen tubules. It is recommended to increase the EDTA concentration with a slightly longer exposure time to ensure complete dissolving of the calcium-alginate within the gelled structures after the collagen is completely gelled via incubation temperatures. The structure should be thoroughly rinsed with PBS 1X and should be hooked up to a flow input and output to ensure no deflation or left over CaCl_2 within the internal channel.

Overall, the viability of cells within the tubule structures were fairly consistent, albeit from 24 hours to 72 hours was not statistically significant. Considering the differences between morphologies within and outside of the tubules structure, an investigation to determine gene expression differences, and differences in present hormones would aid in the process of maintaining and ensuring tissue development. Such investigations could also foretell the need of hormone additions to tubule structures in order to guarantee proper cell function which is linked to morphology. Cells within the tubule structures, despite showing signs of enlargement, did not truly proliferate in mass like that of the external cells. It could improve the generation of

capillary/macro-capillary structures to seed cells internally and allow for attachment to some degree to then be proliferated within the structure as a singular layer. From this, cells can be interacting with a flow and studies of cell morphology and gene expression could be done to see which are most prominent in organizing structures. Alignment, migration, and vWF found in the cell populace around the tubule structure shows that utilizing the tubules as reference structures, aka as a physical barrier/ usable hydrogel matrix, may be better suited to generate the initial vessel structure of endothelial cells rather than bioink seeded with cells.

As a supplement to this thesis, a device is design to theoretically maintain the tubule structure. This device design is meant to take into account the need of the structure to be perfused after incubation, interact with cells, and allow for added bioinks with other cell types for possible thick tissues all while being able to be maintained in incubation and stackable.

REFERENCES

- Antoshin, A. A., Fedyakov, M. D., Sobolevskaya, M. S., Churbanov, S. N., Minaev, N. V., Shpichka, A. I., & Timashev, P. S. (2018, 2018). Applying LIFT-technology for vasculature formation in tissue and organ engineering.
- Attalla, R., Puersten, E., Jain, N., & Selvaganapathy, P. R. (2018). 3D bioprinting of heterogeneous bi- and tri-layered hollow channels within gel scaffolds using scalable multi-axial microfluidic extrusion nozzle. *Biofabrication*, 11(1), 015012. <https://doi.org/10.1088/1758-5090/aaf7c7>
- Axpe, E., & Oyen, M. L. (2016, Nov 25). Applications of Alginate-Based Bioinks in 3D Bioprinting. *Int J Mol Sci*, 17(12). <https://doi.org/10.3390/ijms17121976>
- Bishop, E. S., Mostafa, S., Pakvasa, M., Luu, H. H., Lee, M. J., Wolf, J. M., Ameer, G. A., He, T. C., & Reid, R. R. (2017, Dec). 3-D bioprinting technologies in tissue engineering and regenerative medicine: Current and future trends. *Genes Dis*, 4(4), 185-195. <https://doi.org/10.1016/j.gendis.2017.10.002>
- Bridoux, A., Mousa, S. A., & Samama, M. M. (2012, Jun). Pro- and anti-angiogenic agents. *J Mal Vasc*, 37(3), 132-139. <https://doi.org/10.1016/j.jmv.2012.02.002>
- Browning, M. B., Guiza, V., Russell, B., Rivera, J., Cereceres, S., Hook, M., Hahn, M. S., & Cosgriff-Hernandez, E. M. (2014, Dec). Endothelial cell response to chemical, biological, and physical cues in bioactive hydrogels. *Tissue Eng Part A*, 20(23-24), 3130-3141. <https://doi.org/10.1089/ten.TEA.2013.0602>
- Campbell, P. G., & Weiss, L. E. (2007). Tissue engineering with the aid of inkjet printers. *Expert Opinion on Biological Therapy*, 7(8), 1123-1127. <https://doi.org/10.1517/14712598.7.8.1123>

- Catros, S., Guillotin, B., Bačáková, M., Fricain, J.-C., & Guillemot, F. (2011). Effect of laser energy, substrate film thickness and bioink viscosity on viability of endothelial cells printed by Laser-Assisted Bioprinting. *Applied Surface Science*, 257(12), 5142-5147. <https://doi.org/10.1016/j.apsusc.2010.11.049>
- Chouinard, J. A., Gagnon, S., Couture, M. G., Lévesque, A., & Vermette, P. (2009). Design and validation of a pulsatile perfusion bioreactor for 3D high cell density cultures. *Biotechnology and Bioengineering*, 104(6), 1215-1223. <https://doi.org/10.1002/bit.22477>
- Christensen, K., Xu, C., Chai, W., Zhang, Z., Fu, J., & Huang, Y. (2015, May). Freeform inkjet printing of cellular structures with bifurcations. *Biotechnol Bioeng*, 112(5), 1047-1055. <https://doi.org/10.1002/bit.25501>
- Correa, S. O., Luo, X., & Raub, C. B. (2020). Microfluidic fabrication of stable collagen microgels with aligned microstructure using flow-driven co-deposition and ionic gelation. *Journal of Micromechanics and Microengineering*, 30(8). <https://doi.org/10.1088/1361-6439/ab8ebf>
- Cui, X., & Boland, T. (2009, Oct). Human microvasculature fabrication using thermal inkjet printing technology. *Biomaterials*, 30(31), 6221-6227. <https://doi.org/10.1016/j.biomaterials.2009.07.056>
- Dababneh, A. B., & Ozbolat, I. T. (2014). Bioprinting Technology: A Current State-of-the-Art Review. *Journal of Manufacturing Science and Engineering*, 136(6). <https://doi.org/10.1115/1.4028512>
- Datta, P., Ayan, B., & Ozbolat, I. T. (2017, Mar 15). Bioprinting for vascular and vascularized tissue biofabrication. *Acta Biomater*, 51, 1-20. <https://doi.org/10.1016/j.actbio.2017.01.035>
- Derakhshanfar, S., Mbeleck, R., Xu, K., Zhang, X., Zhong, W., & Xing, M. (2018, Jun). 3D bioprinting for biomedical devices and tissue engineering: A review of recent trends and advances. *Bioact Mater*, 3(2), 144-156. <https://doi.org/10.1016/j.bioactmat.2017.11.008>
- Dorgau, B., Felemban, M., Hilgen, G., Kiening, M., Zerti, D., Hunt, N. C., Doherty, M., Whitfield, P., Hallam, D., White, K., Ding, Y., Krasnogor, N., Al-Aama, J., Asfour, H. Z., Sernagor, E., & Lako, M. (2019, Apr). Decellularised extracellular matrix-derived

peptides from neural retina and retinal pigment epithelium enhance the expression of synaptic markers and light responsiveness of human pluripotent stem cell derived retinal organoids. *Biomaterials*, 199, 63-75. <https://doi.org/10.1016/j.biomaterials.2019.01.028>

Fernandez-Godino, R., Bujakowska, K. M., & Pierce, E. A. (2018, Jan 1). Changes in extracellular matrix cause RPE cells to make basal deposits and activate the alternative complement pathway. *Hum Mol Genet*, 27(1), 147-159. <https://doi.org/10.1093/hmg/ddx392>

Frantz, C., Stewart, K. M., & Weaver, V. M. (2010, Dec 15). The extracellular matrix at a glance. *J Cell Sci*, 123(Pt 24), 4195-4200. <https://doi.org/10.1242/jcs.023820>

Frenguelli, L., Zhang, Z., Chikh, L., Al-Akkad, W., Rombouts, K., Gatenholm, E., Pinzani, M., Martinez, H., & Mazza, G. (2018). 3D bio-printing of human hepatic tissue using human liver extracellular matrix as tissue-specific bioink. *Journal of Hepatology*, 68. [https://doi.org/10.1016/s0168-8278\(18\)30331-3](https://doi.org/10.1016/s0168-8278(18)30331-3)

Gao, Q., He, Y., Fu, J.-Z., Liu, A., & Ma, L. (2015). Coaxial nozzle-assisted 3D bioprinting with built-in microchannels for nutrients delivery. *Biomaterials*, 61, 203-215. <https://doi.org/10.1016/j.biomaterials.2015.05.031>

Gao, Q., He, Y., Fu, J. Z., Liu, A., & Ma, L. (2015, Aug). Coaxial nozzle-assisted 3D bioprinting with built-in microchannels for nutrients delivery. *Biomaterials*, 61, 203-215. <https://doi.org/10.1016/j.biomaterials.2015.05.031>

Gibson, I., Rosen, D., & Stucker, B. (2015). *Additive Manufacturing Technologies* (2 ed.). Springer-Verlag New York. <https://doi.org/10.1007/978-1-4939-2113-3>

Gillies, A. R., & Lieber, R. L. (2011). Structure and function of the skeletal muscle extracellular matrix. *Muscle & Nerve*, n/a-n/a. <https://doi.org/10.1002/mus.22094>

Guillemot, F., Souquet, A., Catros, S., Guillotin, B., Lopez, J., Faucon, M., Pippenger, B., Bareille, R., Remy, M., Bellance, S., Chabassier, P., Fricain, J. C., & Amedee, J. (2010, Jul). High-throughput laser printing of cells and biomaterials for tissue engineering. *Acta Biomater*, 6(7), 2494-2500. <https://doi.org/10.1016/j.actbio.2009.09.029>

- Hoch, E., Tovar, G. E., & Borchers, K. (2014, Nov). Bioprinting of artificial blood vessels: current approaches towards a demanding goal. *Eur J Cardiothorac Surg*, 46(5), 767-778. <https://doi.org/10.1093/ejcts/ezu242>
- Hong, S., Song, S. J., Lee, J. Y., Jang, H., Choi, J., Sun, K., & Park, Y. (2013, Aug). Cellular behavior in micropatterned hydrogels by bioprinting system depended on the cell types and cellular interaction. *J Biosci Bioeng*, 116(2), 224-230. <https://doi.org/10.1016/j.jbiosc.2013.02.011>
- Hoying, J. B., & Williams, S. K. (2015). Biofabrication of Vascular Networks. In *Essentials of 3D Biofabrication and Translation* (pp. 317-335). <https://doi.org/10.1016/b978-0-12-800972-7.00019-0>
- Huang, Y., Zhang, X. F., Gao, G., Yonezawa, T., & Cui, X. (2017, Aug). 3D bioprinting and the current applications in tissue engineering. *Biotechnol J*, 12(8). <https://doi.org/10.1002/biot.201600734>
- Janson, I. A., & Putnam, A. J. (2015, Mar). Extracellular matrix elasticity and topography: material-based cues that affect cell function via conserved mechanisms. *J Biomed Mater Res A*, 103(3), 1246-1258. <https://doi.org/10.1002/jbm.a.35254>
- Ji, J., Zhang, D., Wei, W., Shen, B., Zhang, Y., Wang, Y., Tang, Z., Ni, N., Sun, H., Liu, J., Fan, X., & Gu, P. (2018, Jan). Decellularized matrix of adipose-derived mesenchymal stromal cells enhanced retinal progenitor cell proliferation via the Akt/Erk pathway and neuronal differentiation. *Cytotherapy*, 20(1), 74-86. <https://doi.org/10.1016/j.jcyt.2017.08.019>
- Jia, W., Gungor-Ozkerim, P. S., Zhang, Y. S., Yue, K., Zhu, K., Liu, W., Pi, Q., Byambaa, B., Dokmeci, M. R., Shin, S. R., & Khademhosseini, A. (2016, Nov). Direct 3D bioprinting of perfusable vascular constructs using a blend bioink. *Biomaterials*, 106, 58-68. <https://doi.org/10.1016/j.biomaterials.2016.07.038>
- Jose, R. R., Rodriguez, M. J., Dixon, T. A., Omenetto, F., & Kaplan, D. L. (2016). Evolution of Bioinks and Additive Manufacturing Technologies for 3D Bioprinting. *ACS Biomaterials Science & Engineering*, 2(10), 1662-1678. <https://doi.org/10.1021/acsbiomaterials.6b00088>

- Kang, H. W., Lee, S. J., Ko, I. K., Kengla, C., Yoo, J. J., & Atala, A. (2016, Mar). A 3D bioprinting system to produce human-scale tissue constructs with structural integrity. *Nat Biotechnol*, 34(3), 312-319. <https://doi.org/10.1038/nbt.3413>
- Kauly, T., Kaufman-Francis, K., Lesman, A., & Levenberg, S. (2009, Jun). Vascularization--the conduit to viable engineered tissues. *Tissue Eng Part B Rev*, 15(2), 159-169. <https://doi.org/10.1089/ten.teb.2008.0193>
- Kawecki, F., Clafshenkel, W. P., Auger, F. A., Bourget, J. M., Fradette, J., & Devillard, R. (2018, Apr 30). Self-assembled human osseous cell sheets as living biopapers for the laser-assisted bioprinting of human endothelial cells. *Biofabrication*, 10(3), 035006. <https://doi.org/10.1088/1758-5090/aabd5b>
- Kengla, C., Atala, A., & Lee, S. J. (2015). Bioprinting of Organoids. In *Essentials of 3D Biofabrication and Translation* (pp. 271-282). <https://doi.org/10.1016/b978-0-12-800972-7.00015-3>
- Keriquel, V., Oliveira, H., Remy, M., Ziane, S., Delmond, S., Rousseau, B., Rey, S., Catros, S., Amedee, J., Guillemot, F., & Fricain, J. C. (2017, May 11). In situ printing of mesenchymal stromal cells, by laser-assisted bioprinting, for in vivo bone regeneration applications. *Sci Rep*, 7(1), 1778. <https://doi.org/10.1038/s41598-017-01914-x>
- Kerouredan, O., Bourget, J. M., Remy, M., Crauste-Manciet, S., Kalisky, J., Catros, S., Thebaud, N. B., & Devillard, R. (2019, Feb 12). Micropatterning of endothelial cells to create a capillary-like network with defined architecture by laser-assisted bioprinting. *J Mater Sci Mater Med*, 30(2), 28. <https://doi.org/10.1007/s10856-019-6230-1>
- Kerouredan, O., Hakobyan, D., Remy, M., Ziane, S., Dusserre, N., Fricain, J. C., Delmond, S., Thebaud, N. B., & Devillard, R. (2019, Jul 3). In situ prevascularization designed by laser-assisted bioprinting: effect on bone regeneration. *Biofabrication*, 11(4), 045002. <https://doi.org/10.1088/1758-5090/ab2620>
- Kim, B. S., Kwon, Y. W., Kong, J. S., Park, G. T., Gao, G., Han, W., Kim, M. B., Lee, H., Kim, J. H., & Cho, D. W. (2018, Jun). 3D cell printing of in vitro stabilized skin model and in vivo pre-vascularized skin patch using tissue-specific extracellular matrix bioink: A step towards advanced skin tissue engineering. *Biomaterials*, 168, 38-53. <https://doi.org/10.1016/j.biomaterials.2018.03.040>

- Kim, J. H., Seol, Y. J., Ko, I. K., Kang, H. W., Lee, Y. K., Yoo, J. J., Atala, A., & Lee, S. J. (2018, Aug 17). 3D Bioprinted Human Skeletal Muscle Constructs for Muscle Function Restoration. *Sci Rep*, 8(1), 12307. <https://doi.org/10.1038/s41598-018-29968-5>
- Kolesky, D. B., Homan, K. A., Skylar-Scott, M. A., & Lewis, J. A. (2016). Three-dimensional bioprinting of thick vascularized tissues. *Proceedings of the National Academy of Sciences*, 113(12), 3179-3184. <https://doi.org/10.1073/pnas.1521342113>
- Maiullari, F., Costantini, M., Milan, M., Pace, V., Chirivì, M., Maiullari, S., Rainer, A., Baci, D., Marei, H. E.-S., Seliktar, D., Gargioli, C., Bearzi, C., & Rizzi, R. (2018). A multi-cellular 3D bioprinting approach for vascularized heart tissue engineering based on HUVECs and iPSC-derived cardiomyocytes. *Scientific Reports*. <https://doi.org/10.1038/s41598-018-31848-x>
- Norotte, C., Marga, F. S., Niklason, L. E., & Forgacs, G. (2009, Oct). Scaffold-free vascular tissue engineering using bioprinting. *Biomaterials*, 30(30), 5910-5917. <https://doi.org/10.1016/j.biomaterials.2009.06.034>
- Ong, C. S., Nam, L., Ong, K., Krishnan, A., Huang, C. Y., Fukunishi, T., & Hibino, N. (2018). 3D and 4D Bioprinting of the Myocardium: Current Approaches, Challenges, and Future Prospects. *Biomed Res Int*, 2018, 6497242. <https://doi.org/10.1155/2018/6497242>
- Park, J. Y., Choi, J. C., Shim, J. H., Lee, J. S., Park, H., Kim, S. W., Doh, J., & Cho, D. W. (2014, Sep). A comparative study on collagen type I and hyaluronic acid dependent cell behavior for osteochondral tissue bioprinting. *Biofabrication*, 6(3), 035004. <https://doi.org/10.1088/1758-5082/6/3/035004>
- Rajan, A. M., Ma, R. C., Kocha, K. M., Zhang, D. J., & Huang, P. (2020). Dual function of perivascular fibroblasts in vascular stabilization in zebrafish. <https://doi.org/10.1101/2020.04.27.063792>
- Roopavath, U. K., & Kalaskar, D. M. (2017). Introduction to 3D printing in medicine. In *3D Printing in Medicine* (pp. 1-20). <https://doi.org/10.1016/b978-0-08-100717-4.00001-6>
- Roseti, L., Cavallo, C., Desando, G., Parisi, V., Petretta, M., Bartolotti, I., & Grigolo, B. (2018). Three-Dimensional Bioprinting of Cartilage by the Use of Stem Cells: A Strategy to Improve Regeneration. *Materials*, 11(9), 1749. <https://doi.org/10.3390/ma11091749>

- Sarker, M. D., Naghieh, S., Sharma, N. K., & Chen, X. (2018, Oct). 3D biofabrication of vascular networks for tissue regeneration: A report on recent advances. *J Pharm Anal*, 8(5), 277-296. <https://doi.org/10.1016/j.jpha.2018.08.005>
- Sawdon, M., & Kirkman, E. (2020). Capillary dynamics and the interstitial fluid–lymphatic system. *Anaesthesia & Intensive Care Medicine*, 21(7), 356-362. <https://doi.org/10.1016/j.mpaic.2020.04.006>
- Singh, M., Haverinen, H. M., Dhagat, P., & Jabbour, G. E. (2010, Feb 9). Inkjet printing-process and its applications. *Adv Mater*, 22(6), 673-685. <https://doi.org/10.1002/adma.200901141>
- Skardal, A. (2015). Bioprinting Essentials of Cell and Protein Viability. In *Essentials of 3D Biofabrication and Translation* (pp. 1-17). <https://doi.org/10.1016/b978-0-12-800972-7.00001-3>
- Sooppan, R., Paulsen, S. J., Han, J., Ta, A. H., Dinh, P., Gaffey, A. C., Venkataraman, C., Trubelja, A., Hung, G., Miller, J. S., & Atluri, P. (2016). In Vivo Anastomosis and Perfusion of a Three-Dimensionally-Printed Construct Containing Microchannel Networks. *Tissue Engineering Part C: Methods*, 22(1), 1-7. <https://doi.org/10.1089/ten.tec.2015.0239>
- Streuli, C. (1999). Extracellular matrix remodeling and cellular differentiation. *Current Opinion in Cell Biology*, 11, 634-640.
- Sundaramurthi, D., Rauf, S., & Hauser, C. (2016). 3D bioprinting technology for regenerative medicine applications. *International Journal of Bioprinting*, 2(2). <https://doi.org/10.18063/ijb.2016.02.010>
- Tarassoli, S. P., Jessop, Z. M., Al-Sabah, A., Gao, N., Whitaker, S., Doak, S., & Whitaker, I. S. (2018, May). Skin tissue engineering using 3D bioprinting: An evolving research field. *J Plast Reconstr Aesthet Surg*, 71(5), 615-623. <https://doi.org/10.1016/j.bjps.2017.12.006>
- Williams, S. K., & Hoying, J. B. (2015). Bioinks for Bioprinting. In K. Turksen (Ed.), *Bioprinting in Regenerative Medicine* (pp. 1-31). Springer International Publishing. https://doi.org/10.1007/978-3-319-21386-6_1

- Witowski, J., Sitkowski, M., Zuzak, T., Coles-Black, J., Chuen, J., Major, P., & Pdzwiatr, M. (2018, Sep). From ideas to long-term studies: 3D printing clinical trials review. *Int J Comput Assist Radiol Surg*, 13(9), 1473-1478. <https://doi.org/10.1007/s11548-018-1793-8>
- Wu, P. K., & Ringeisen, B. R. (2010, Mar). Development of human umbilical vein endothelial cell (HUVEC) and human umbilical vein smooth muscle cell (HUVSMC) branch/stem structures on hydrogel layers via biological laser printing (BioLP). *Biofabrication*, 2(1), 014111. <https://doi.org/10.1088/1758-5082/2/1/014111>
- Xu, T., Zhao, W., Zhu, J. M., Albanna, M. Z., Yoo, J. J., & Atala, A. (2013, Jan). Complex heterogeneous tissue constructs containing multiple cell types prepared by inkjet printing technology. *Biomaterials*, 34(1), 130-139. <https://doi.org/10.1016/j.biomaterials.2012.09.035>
- Yu, Y., Zhang, Y., Martin, J. A., & Ozbolat, I. T. (2013, Sep). Evaluation of cell viability and functionality in vessel-like bioprintable cell-laden tubular channels. *J Biomech Eng*, 135(9), 91011. <https://doi.org/10.1115/1.4024575>
- Zhang, Y., Yu, Y., Akkouch, A., Dababneh, A., Dolati, F., & Ozbolat, I. T. (2015). In vitro study of directly bioprinted perfusable vasculature conduits. *Biomaterials Science*, 3(1), 134-143. <https://doi.org/10.1039/c4bm00234b>
- Zhang, Y., Yu, Y., Chen, H., & Ozbolat, I. T. (2013). Characterization of printable cellular micro-fluidic channels for tissue engineering. *Biofabrication*, 5(2), 025004. <https://doi.org/10.1088/1758-5082/5/2/025004>
- Zhang, Y. S., Pi, Q., & van Genderen, A. M. (2017, Aug 11). Microfluidic Bioprinting for Engineering Vascularized Tissues and Organoids. *J Vis Exp*(126). <https://doi.org/10.3791/55957>
- Zhang, Y. S., Yue, K., Aleman, J., Moghaddam, K. M., Bakht, S. M., Yang, J., Jia, W., Dell'Erba, V., Assawes, P., Shin, S. R., Dokmeci, M. R., Oklu, R., & Khademhosseini, A. (2017, Jan). 3D Bioprinting for Tissue and Organ Fabrication. *Ann Biomed Eng*, 45(1), 148-163. <https://doi.org/10.1007/s10439-016-1612-8>

Zhu, W., Qu, X., Zhu, J., Ma, X., Patel, S., Liu, J., Wang, P., Lai, C. S., Gou, M., Xu, Y., Zhang, K., & Chen, S. (2017, Apr). Direct 3D bioprinting of prevascularized tissue constructs with complex microarchitecture. *Biomaterials*, 124, 106-115.
<https://doi.org/10.1016/j.biomaterials.2017.01.042>

BIOGRAPHICAL SKETCH

Victoria Jade Perez, nicknamed Tori, is a student at the University of Texas Rio Grande Valley. One of three siblings, she grew up around a family with many interests. She was in the top 10% of the student body in her primary years of schooling and was committed to many clubs and after school activities that included Mu Alpha Theta, Honor Society, Tri-M Music Club, and Orchestral offices. Victoria was ranked principle double bassist in the state of Texas and received multiple medals for state level solo and ensembles. Receiving multiple awards for both music and education, Victoria moved onto her secondary education in which she graduated from UTRGV with a Bachelor of Science in Biology with a double minor in Chemistry and Physics. Her work is centered around biology and manufacturing engineering. She has earned a graduate degree in Manufacturing Engineering as of August 2021 and can be contacted at victoria.jadeperez@gmail.com.